The Hubbard chain at finite temperatures: ab initio calculations of Tomonaga-Luttinger liquid properties

G. Jüttner*, A. Klümper†, J. Suzuki‡

Universität zu Köln
Institut für Theoretische Physik
Zülpicher Str. 77
D-50937, Germany

October 1997

Abstract

We present a novel treatment of finite temperature properties of the one-dimensional Hubbard model. Our approach is based on a Trotter-Suzuki mapping utilizing Shastry's classical model and a subsequent investigation of the quantum transfer matrix. We derive non-linear integral equations for three auxiliary functions which have a clear physical interpretation of elementary excitations of spin type and charge excitations in lower and upper Hubbard bands. This allows for a transparent analytical study of certain limiting cases as well as for precise numerical investigations. We present data for the specific heat, magnetic and charge susceptibilities for various particle densities and coupling strengths U. The structure exposed by these curves is discussed in terms of the elementary charge and spin excitations. Special emphasis is placed on the study of the low-temperature behavior within our ab initio approach confirming the scaling predictions by Tomonaga-Luttinger liquid theory. In addition we make contact with the "dressed energy" formalism established for the analysis of ground state properties.

*e-mail: gj@thp.uni-koeln.de
†e-mail: kluemper@thp.uni-koeln.de
‡e-mail: suz@hep1.c.u-tokyo.ac.jp, Permanent address: Institute of Physics, University of Tokyo at Komaba

1 Introduction

The Hubbard model represents the most fundamental model for highly correlated electron systems. It has therefore attracted much attention since its formulation. Triggered by the discovery of high T_c superconductivity, correlation effects of the model have been of strong recent interest.

For the problem in one spatial dimension an exact solution is available via the Bethe ansatz [1]. It clarified the Mott insulator nature of the itinerant electron system at half-filling in 1D. The extensive list of investigations of zero temperature properties ranges from studies of the elementary excitations [2, 3, 4, 5], over magnetic properties [6] to studies of correlation functions in the strong coupling limit [7]. Recently, the large group of symmetries of the Hubbard model was analyzed in [8, 9, 10, 11]. It was, however, almost 20 years after the discovery of the exact solution that various properties like asymptotics of correlations functions at $T = 0$ have been investigated by using results of conformal field theory. The Tomonaga-Luttinger liquid properties of the one-dimensional model have been shown not only at a qualitative but also at satisfactory quantitative level [12, 13, 14, 15].

In this report, we address the problem of the Hubbard model at finite temperatures. In fact, soon after the seminal solution [1], a thermodynamic formulation was set up through the string hypothesis approach [16]. It results into infinitely many ($\infty \times \infty$) coupled nonlinear integral equations for infinitely many unknown functions. Obviously, quantitative studies of such equations need much effort and were performed only relatively recently (also about 20 years after the thermodynamical formulation!) [17, 18]. Still, the explicit calculation allowed for only 2 (!) bound charge rapidities and 15-30 spin rapidities, while the original equations contain $\infty \times \infty$ rapidities.

Here we attack the problem via a completely different approach developed recently which avoids the computational complications and also renders correlations lengths at finite temperatures accessible. We make use of a general equivalence theorem between d-dimensional quantum systems at finite temperatures and $d + 1$-dimensional classical systems [19], thus we employ a convenient mapping to a two-dimensional classical model. The evaluation of the free energy then reduces to finding the largest eigenvalue of the so-called quantum transfer matrix (QTM) [19, 20, 21, 22, 23, 24, 25, 26, 27, 28]. The crucial observation is the existence of a commuting family of QTMs labeled by one complex parameter (spectral parameter) [25, 26, 29, 30, 31]. This makes the meaning of integrability manifest, and allows for the investigation of thermodynamics through the study of the analytical properties of suitably defined auxiliary functions on the complex space of the spectral parameter. One of the most practical advantages in this novel formulation is the fact that one has to deal with only a finite number of auxiliary functions and nonlinear integral equations among them. Therefore, we can expect results with higher numerical precision. Furthermore, the involved auxiliary functions have clear physical interpretations in terms of elementary excitations at $T = 0$.

Such a strategy has been successfully applied to several interesting models including the spin 1/2 XYZ model and derivates [25, 26, 28, 27], the integrable $t-J$ model [29, 30], the supersymmetric U model [31], and (with limited success) to the Hubbard model

[32, 23, 33]. The main restriction of the previous work on the Hubbard chain [23, 33] is the limitation to the case of half-filling. For any finite doping the resultant equations appeared to be numerically ill-posed. Here we want to overcome the technical difficulties and derive a set of equations that allow for convenient (numerical) studies and clear analytical insight for all particle densities. Before doing so, we want to remind of the remarkable differences in comparison to other solvable models. The $R-$matrix for the classical analogue ("Shastry's model") [34, 35, 36] does not possess the difference property of rapidities. Therefore, the intertwiner depends on two spectral parameters, not only on the difference. Such violations are only known for Shastry's model and the chiral Potts model. In view of analyticity, the Hubbard model is also quite unique. One can easily recognize this by comparing the Bethe ansatz equations (BAE) at $T = 0$ for the Hubbard model [1], with, for instance, those for the integrable $t-J$ model [37, 38, 39]. In both cases there are two kinds of BAE roots corresponding to charge and spin degrees of freedom. However for the integrable $t-J$ model both types of roots vary from $-\infty$ to ∞, while the charge-rapidities for the Hubbard model only vary from $-\pi$ to π with a corresponding periodicity. This different character of the BAE roots brings about branch cuts in a complex parameter plane as we will see below. The roots show an exotic behavior: they flow from one Riemann sheet to the other with changing temperature.

Despite these difficulties, we will show our strategy is successfully applicable to the Hubbard model (and finally overcomes the technical problems still left in the earlier approach [33]). With a careful choice of auxiliary functions, we can completely encode the information about zeros in both sheets. They are shown to have close relation to the physical excitations of holons and spinons in the $T \to 0$ limit. This limit will be studied in quite some detail as it allows for a first principles derivation of Tomonaga-Luttinger liquid properties at low but finite temperatures. Several quantities of physical interests are evaluated with high numerical precisions for wide ranges of temperatures and fillings.

This paper is organized as follows. In Section 2 we present the mapping of the Hubbard chain at finite temperature to a two-dimensional classical system with integrable QTM. In Section 3 the eigenvalue equations for the QTM are derived which are cast into a difference type form in Section 4. Section 5 is devoted to the derivation of non-linear integral equations for Hubbard interactions $U > 0$. In Section 6 the integral equations are investigated numerically and the results are discussed. Section 7 deals with the analytical study of various limiting cases, notably the low-temperature asymptotics. In Section 8 we present our summary and outlook. The derivation of the integral form of the QTM eigenvalue is deferred to Appendix A.

2 Shastry's Model as a classical analogue of the 1D Hubbard Model

In the novel formalism, it is essential to deal with the two dimensional classical counterpart. Fortunately, Shastry has already found two classical versions for the Hubbard model [40, 34]. For the latter model, a proof of the Yang-Baxter integrability has been given in

a recent analysis [41] by the use of the tetrahedron algebra. As the Yang-Baxter relation makes the finite temperature analysis much easier, we adopt the latter version here.

We sketch the essential properties of the model. The Hubbard model describes a lattice fermion system with electron hopping term and on-site Coulomb repulsion with Hamiltonian

$$\begin{aligned} \mathcal{H}_{\rm Hubbard} &= \sum_{i=1}^{L} \left\{ \sum_{\sigma=\pm} -(c^{\dagger}_{i+1,\sigma} c_{i,\sigma} + c^{\dagger}_{i,\sigma} c_{i+1,\sigma}) + U(n_{i,-} - \tfrac{1}{2})(n_{i,+} - \tfrac{1}{2}) \right\} \\ &+ \mathcal{H}_{\rm external}. \end{aligned} \tag{1}$$

The external field term $\mathcal{H}_{\rm external} = -\sum_i [\mu(n_{i,+}+n_{i,-}) + H/2(n_{i,+}-n_{i,-})]$ will be omitted for the time being. According to [34], it is easier to find a classical analogue after performing the Jordan-Wigner transformations for electrons in 1D. The resultant spin Hamiltonian is

$$\begin{aligned} \mathcal{H}_L &= \sum_{n=1}^{L} \mathcal{H}_{n,n+1}, \\ \mathcal{H}_{n,n+1} &= (\sigma^+_n \sigma^-_{n+1} + \sigma^+_{n+1}\sigma^-_n) + (\tau^+_n \tau^-_{n+1} + \tau^+_{n+1}\tau^-_n) + \tfrac{U}{4}\,\sigma^z_n \tau^z_n, \end{aligned} \tag{2}$$

where L denotes the chain length of the system. Note that we are now imposing periodic boundary conditions for the spin system ($\sigma_1(\tau_1) = \sigma_{L+1}(\tau_{L+1})$). This does not give the periodic boundary conditions for the underlying electron system. The differences in boundary conditions, however, will not affect thermodynamic quantities like the specific heat.

For the counterpart in two dimensions, we consider two double-layer square lattices, say a σ and a τ lattice. Each edge possesses a local variable $\pm$ and each vertex satisfies the ice rule. The vertex weights consist of contributions from both intra and inter lattice interactions. The intra part is given by the product of vertex weights of the free-fermion six vertex model: $\ell_{1,2}(u) = \ell^{\sigma}_{1,2}(u) \otimes \ell^{\tau}_{1,2}(u)$ where

$$\ell^{\sigma}_{1,2}(u) = \frac{a(u)+b(u)}{2} + \frac{a(u)-b(u)}{2}\sigma^z_1\sigma^z_2 + c(\sigma^+_1\sigma^-_2 + \sigma^-_1\sigma^+_2) \tag{3}$$

and $a(u) = \cos(u)$, $b(u) = \sin(u)$, $c(u) = 1$. Taking account of inter-layer interactions, the following local vertex weight operator (denoted by S) is found [34]

$$\begin{aligned} S_{1,2}(v,u) &= \cos(u+v)\,\cosh(h(v,U) - h(u,U))\,\ell_{1,2}(v-u) \\ &+ \cos(v-u)\,\sinh(h(v,U) - h(u,U))\,\ell_{1,2}(u+v)\,\sigma^z_2\tau^z_2 \end{aligned}$$

where $\sinh 2h(u,U) := Ua(u)b(u)/2$. The Yang-Baxter relation for triple S matrices is proved in [41]. The commutativity of the row-to-row transfer matrix,

$$\mathcal{T}(u) := \overleftarrow{\prod_i} S_{i,g}(u,0) \tag{4}$$

is the direct consequence.

The S matrix and $\mathcal{H}$ are related by the expansion in small spectral parameters,

$$S_{1,2}(u,0) = S_{1,2}(0,-u) \sim P(1 + u\mathcal{H}_{1,2} + O(u^2)), \tag{5}$$

where P denotes the permutation operator, $P(x \otimes y) = y \otimes x$. Once the Yang-Baxter relation is established, we can apply our machinery for thermodynamics. Here we summarize the necessary formulas, see [30] for details. We define $R_{1,2}(u,v) = S_{1,2}(v,u)|_{U\to -U}$, and introduce $\widetilde{R}(u,v)$ and $\overline{R}(u,v)$ by clockwise and anticlockwise 90° rotations of $R_{1,2}(u,v)$. We further introduce an auxiliary transfer matrix $\overline{\mathcal{T}}(u)$ made of Boltzmann weights $\overline{R}(0,-u)$. The partition function is given by

$$Z = \lim_{L\to\infty} \mathrm{Tr} e^{-\beta \mathcal{H'}_L} = \lim_{L\to\infty} \lim_{N\to\infty} \mathrm{Tr}\, [\mathcal{T}(u)\overline{\mathcal{T}}(u)]^{N/2}|_{u=\beta/N} \tag{6}$$

where $\mathcal{H'}_L$ differs from $\mathcal{H}_L$ by the sublattice gauge transformation, $c_{n,\sigma} \to (-1)^n c_{n,\sigma}$ which does not affect thermodynamic behaviors. We regard the resulting system as a fictitious two-dimensional model on a $L \times N$ square lattice, where N is the extension in the fictitious (imaginary time) direction, sometimes referred to as the Trotter number. Now by looking at the system in a 90° rotated frame, it is natural to define the "quantum transfer matrix" (QTM) by

$$\mathcal{T}_{\mathrm{QTM}}(u,v) = \bigotimes^{N/2} R(-u,v) \otimes \widetilde{R}(v,u). \tag{7}$$

The interchangeability of the two limits ($L, N \to \infty$) leads to the following expression,

$$Z = \lim_{N\to\infty} \lim_{L\to\infty} \mathrm{Tr} \left[\mathcal{T}_{\mathrm{QTM}}\left(u = \frac{\beta}{N}, 0\right)\right]^L. \tag{8}$$

There is a gap between the largest and the second largest eigenvalues of $\mathcal{T}_{\mathrm{QTM}}(u,0)$ for finite β. Therefore, we have a formula for the free energy per site,

$$f = -k_B T \lim_{N\to\infty} \ln \Lambda_{\max}\left(u = \frac{\beta}{N}, 0\right). \tag{9}$$

where $\Lambda_{\max}(u,0)$ denotes the largest eigenvalue of $\mathcal{T}_{\mathrm{QTM}}(u,0)$. Now the evaluation of the free energy reduces to that of the single eigenvalue $\Lambda_{\max}$. Of course, a sophisticated treatment is necessary in taking the Trotter limit $N \to \infty$ as u now explicitly depends on it. The following sections are devoted to this analysis.

A general comment is in order. It seems somewhat redundant to define $\mathcal{T}_{\mathrm{QTM}}(u,v)$ as we only need the value at $v = 0$. This formulation, however, manifests the integrability structure and the existence of infinitely many conserved quantities. This is best seen in the commutativity of transfer matrices

$$[\mathcal{T}_{\mathrm{QTM}}(u,v), \mathcal{T}_{\mathrm{QTM}}(u,v')] = 0, \tag{10}$$

with fixed u. One can prove this by showing that two QTMs are intertwined by the same R operator as for the row-to-row case. The outline of the proof is graphically demonstrated in Fig.1. The existence of the parameter labeling the family of commuting matrices makes the subsequent analysis much more transparent.

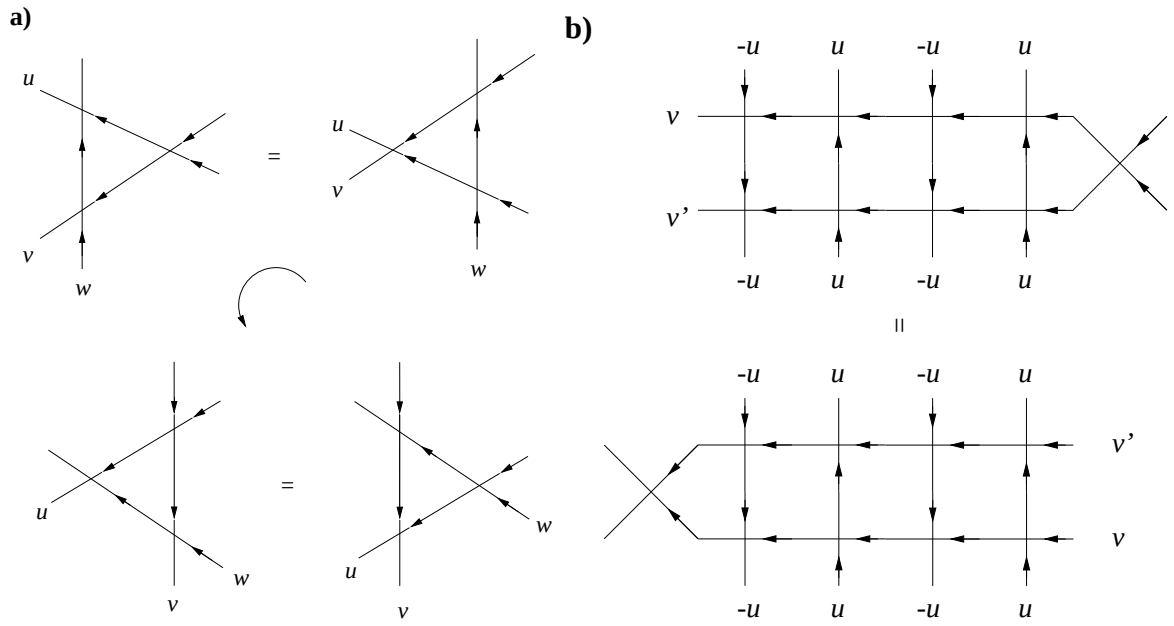

Figure 1: a) Graphical depiction of the fundamental Yang-Baxter equation for R and the associated one for R and $\widetilde{R}$ obtained through rotation. b) "Railroad proof" for the commutation of two QTM's with any spectral parameters v and v'. Due to a) the intertwiner for R vertices is identical to the intertwiner for $\widetilde{R}$ vertices.

3 Diagonalization of the Quantum Transfer Matrix

It has been an issue of current interest to find an explicit algorithm of the diagonalization of the row-to-row transfer matrix of Shastry's model or its fermion version. The standard tool in such studies, the quantum inverse scattering method, has been applied and turned out to be successful after elaborate calculations [42]. We also refer to the analytic Bethe ansatz study [43].

Here we want to diagonalize the QTM. At first glance, the diagonalization scheme for this looks quite different from the row-to-row case. The QTM has a complicated inhomogeneous structure seemingly demanding much more effort. Fortunately, this is not true. The crucial observation is, as remarked in the previous section, that QTMs share the same intertwining operator with the row-to-row transfer matrices. In view of QISM, this results into identical operator algebras which allows for the diagonalization of the trace of the monodromy matrix. (Note that we adopt periodic boundaries in the Trotter direction.) Thus, the eigenvalue equation of the QTM involves the same combinations of "dress functions" (in the terminology of the analytic Bethe ansatz) as in the row-to-row case. One only has to replace the vacuum expectation values taking account of the quantum space and the inhomogeneity.

We define state vectors $|i\rangle, i = 1, \cdots, 4$ by

$$|1\rangle = |+,-\rangle, \quad |2\rangle = |+,+\rangle, \quad |3\rangle = |-,-\rangle, \quad |4\rangle = |-,+\rangle. \tag{11}$$

A convenient vacuum in the present study may be $|\Omega\rangle := |1,4,1,4,\cdots,1,4\rangle$. Then the vacuum expectation values read

$$A_i = \langle\Omega|\mathcal{T}_{i,i}|\Omega\rangle = (R^{i,1}_{1,i}(-u,v)R^{4,i}_{i,4}(v,u))^{N/2} \quad i = 1,\cdots,4. \tag{12}$$

Substituting explicit elements for R, we find the relations

$$\begin{aligned}
A_1/A_2 &= \left(\frac{(1-z_-(w)z_+(x))(1-z_+(w)z_+(x))}{(1+z_-(w)z_+(x))(1+z_+(w)z_+(x))}\right)^{N/2} \\
A_2 &= A_3 \\
A_4/A_2 &= \left(\frac{(1+z_-(w)/z_-(x))(1+z_+(w)/z_-(x))}{(1-z_-(w)/z_-(x))(1-z_+(w)/z_-(x))}\right)^{N/2} \\
A_2 &= \left(\frac{\cos^2(u-v)\cos^2(u+v)}{(1+e^{4x})(1+e^{4w})}e^{2h(w)}(\frac{1}{z_-(w)}-\frac{1}{z_-(x)})(z_+(x)+\frac{1}{z_-(w)})\right)^{N/2}
\end{aligned}$$

where we have introduced the parameterizations x, w for v, u,

$$e^{2x} = \tan v, \qquad e^{2w} = \tan u, \tag{13}$$

and the functions

$$z_\pm(x) = e^{2h(x)\pm 2x}, \quad 2h(x) = -\sinh^{-1}\left(\frac{U}{4\cosh 2x}\right). \tag{14}$$

Now that we have the explicit vacuum expectation values, the eigenvalue can be written down directly thanks to the above argument

$$\begin{aligned}
\frac{\Lambda(v)}{A_2} &= e^{\beta(\mu+H/2)}\frac{A_1}{A_2}\prod_{j=1}^m e^{2x}\frac{1+z_jz_-(x)}{1-z_jz_+(x)} \\
&+ e^{2\beta\mu}\prod_{j=1}^m -e^{2x}\frac{1+z_jz_-(x)}{1-z_jz_+(x)}\prod_{\alpha=1}^\ell -\frac{z_-(x)-1/z_-(x)-2iw_\alpha+3U/2}{z_-(x)-1/z_-(x)-2iw_\alpha+U/2} \\
&+ \prod_{j=1}^m -e^{-2x}\frac{1+z_+(x)/z_j}{1-z_-(x)/z_j}\prod_{\alpha=1}^\ell -\frac{z_-(x)-1/z_-(x)-2iw_\alpha-U/2}{z_-(x)-1/z_-(x)-2iw_\alpha+U/2} \\
&+ e^{\beta(\mu-H/2)}\frac{A_4}{A_2}\prod_{j=1}^m e^{-2x}\frac{1+z_+(x)/z_j}{1-z_-(x)/z_j}.
\end{aligned} \tag{15}$$

Note that we imposed a non-vanishing chemical potential and magnetic field at the last stage, as they merely lead to trivial modifications in Λ due to twisted boundary conditions for the QTM [30].

The parameters $\{z_j\}, \{w_\alpha\}$ satisfy the BAE,

$$e^{\beta(\mu-H/2)}\left(\frac{(1+z_-(w)/z_j)(1+z_+(w)/z_j)}{(1-z_-(w)/z_j)(1-z_+(w)/z_j)}\right)^{N/2} = -(-1)^m\prod_{\alpha=1}^{\ell} -\frac{z_j-1/z_j-2iw_\alpha-U/2}{z_j-1/z_j-2iw_\alpha+U/2},$$
$$e^{2\beta\mu}\prod_{j=1}^{m}\frac{z_j-1/z_j-2iw_\alpha+U/2}{z_j-1/z_j-2iw_\alpha-U/2} = -\prod_{\beta=1}^{\ell}\frac{2i(w_\alpha-w_\beta)-U}{2i(w_\alpha-w_\beta)+U}. \tag{16}$$

Here some remarks are in order:

1. Although the validity of expression (15) is a logical consequence, it would be a good exercise to verify this form for one-particle states. For example, we take $\mathcal{T}_{3,4}(\nu)|\Omega\rangle$ as a representative, and calculate its eigenvalue. A standard argument in QISM leads to the following "wanted terms".

$$\begin{aligned}\text{wanted terms } = \Bigg[&A_1\frac{R^{3,1}_{1,3}(v,\nu)}{R^{4,1}_{1,4}(v,\nu)} + A_2\left(\frac{R^{3,2}_{2,3}(v,\nu)}{R^{4,2}_{2,4}(v,\nu)} - \frac{R^{3,2}_{1,4}(v,\nu)R^{4,1}_{2,3}(v,\nu)}{R^{4,2}_{2,4}(v,\nu)R^{4,1}_{1,4}(v,\nu)}\right)\\ &+ A_3\frac{R^{3,3}_{3,3}(v,\nu)}{R^{4,3}_{3,4}(v,\nu)} + A_4\frac{R^{4,4}_{4,4}(\nu,v)}{R^{4,3}_{3,4}(\nu,v)}\Bigg]\mathcal{T}_{3,4}(\nu)|\Omega\rangle\end{aligned} \tag{17}$$

   A straightforward however lengthy calculation shows the coefficient in (17) is equal to (15) with $m=1$, $\ell=0$, $z_1 = z_-(1/2\log(\tan\nu))$.

2. We have verified that (15) gives the largest eigenvalue identical to the one obtained by brute force diagonalizations of finite systems up to $N=6$. The groundstate lies in the sector $m=N$, $\ell=N/2$. For the repulsive case and $\mu=H=0$, z_j's are all on the imaginary axis, while w_α's are real.

3. The free-fermion partition function is easily recovered for $U=0$.

4. Starting from another vacuum $|\Omega'\rangle = |2,3,\cdots\rangle$, one reaches a different expression. The resultant one is actually equivalent after negating U and exchanging $H/2 \leftrightarrow \mu$, namely, after the partial particle-hole transformation.

4 Associated auxiliary problem of difference type

The thermodynamics leading to the free energy is encoded in the solution to the BAE (16) in the limit $N\to\infty$. For finite N it is possible to solve the BAE numerically. However, for large N it is quite complicated to find the numerical solution even for the ground state. Furthermore, in the Trotter limit $N\to\infty$ the roots $\{v_k, w_k\}$ accumulate at infinity. This is similar to other models (Heisenberg model, $t-J$ model) where the solutions of BAE of the QTM tend to the origin [25, 26, 27, 29, 30, 31]. It represents the main problem in

analyzing the limit $N \to \infty$ directly on the basis of the BAE. To overcome this difficulty one can express the solution of the BAE by a system of non-linear integral equations. This has been done for several models [44, 45, 25, 26, 27, 29, 30, 31].

The first problem to be overcome is the involved structure of BAE (16). Upon introducing the quantities

$$s_j = \frac{1}{2i}\left(z_j - \frac{1}{z_j}\right), \tag{18}$$

the equations (16) take a difference form in the rapidities $\{s_j\}, \{w_\alpha\}$:

$$\mathrm{e}^{-\beta(\mu - H/2)}\phi(s_j) = -\frac{q_2(s_j - i\gamma)}{q_2(s_j + i\gamma)}, \tag{19}$$

$$\mathrm{e}^{-2\beta\mu}\frac{q_2(w_\alpha + 2i\gamma)}{q_2(w_\alpha - 2i\gamma)} = -\frac{q_1(w_\alpha + i\gamma)}{q_1(w_\alpha - i\gamma)}, \tag{20}$$

with

$$q_1(s) = \prod_j (s - s_j), \quad q_2(s) = \prod_\alpha (s - w_\alpha), \quad \gamma = \frac{U}{4}, \tag{21}$$

and

$$\phi(s) = \left(\frac{(1 - z_-(w)/z(s))(1 - z_+(w)/z(s))}{(1 + z_-(w)/z(s))(1 + z_+(w)/z(s))}\right)^{N/2}, \tag{22}$$

$$z(s) = is(1 + \sqrt{(1 - 1/s^2)}). \tag{23}$$

The function $z(s)$ possesses two branches. The standard ("first") branch is chosen by the requirement $z(s) \simeq 2is$ for large values of s, and the branch cut line $[-1, 1]$ (corresponding to a cut for $\sqrt{z}$ from $-\infty$ to 0.) We will not refer explicitly to the second branch of $z(s)$ in this work. However, for $\phi(s)$ both branches will be used. In order to distinguish between the first and second one we will use the notation $\phi^+(s)$ and $\phi^-(s)$, respectively.

In Fig.2 the distribution of rapidities s_j is shown for $N \to \infty$. Note that there are infinitely many rapidities on the first (upper) sheet and finitely many on the second (lower) sheet. The number of rapidities on the second sheet is increasing with decreasing temperature thus resulting into a flow from the first to the second sheet.

Note that the general expression (15) is quite complicated, but simplifies considerably at $v = 0$ and $u \to 0$

$$\Lambda(v = 0) = e^{\beta\gamma}(1 + e^{\beta(\mu + H/2)})(1 + e^{\beta(\mu - H/2)})u^N \prod_{j=1}^{m} z_j. \tag{24}$$

Lastly, we want to comment on the difference type property of (20). These equations are "BAE compatible" with the following eigenvalue equation of an "auxiliary transfer matrix"

$$\Lambda^{\mathrm{aux}}(s) = \lambda_1(s) + \lambda_2(s) + \lambda_3(s) + \lambda_4(s), \tag{25}$$

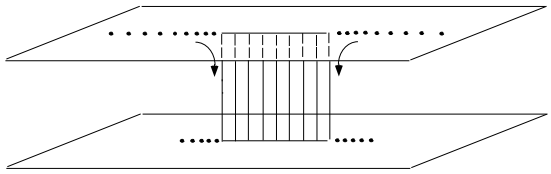

Figure 2: Depiction of the flow of rapidities s_j from the first (upper) Riemann sheet to the second (lower) one for decreasing temperature.

$$\begin{aligned}
\lambda_1(s) &= \mathrm{e}^{\beta(\mu+H/2)}\frac{\phi(s-i\gamma)}{q_1(s-i\gamma)}\,, \quad \lambda_2(s) = \mathrm{e}^{2\beta\mu}\frac{q_2(s-2i\gamma)}{q_2(s)q_1(s-i\gamma)}\,,\\
\lambda_3(s) &= \frac{q_2(s+2i\gamma)}{q_2(s)q_1(s+i\gamma)}, \qquad \lambda_4(s) = \mathrm{e}^{\beta(\mu-H/2)}\frac{1}{\phi(s+i\gamma)\,q_1(s+i\gamma)}\,.
\end{aligned} \tag{26}$$

The reason is obvious, $\Lambda^{\mathrm{aux}}(s)$ is pole free under BAE (20) just like the original QTM. The construction (26) at this point is purely mathematical, however it will be the starting point of the derivation of integral equations in the next section.

5 Non-linear integral equations

In this section we are concerned with the derivation of well posed integral equations equivalent to the nested BAE for the largest eigenvalue of the QTM. (We restrict ourselves to the case $U > 0$ and point out that $U < 0$ is simply obtained via a particle-hole transformation.) We introduce a set of auxiliary functions which satisfy a set of closed functional equations which later on are transformed into integral form. The explicit expression of the functions $\mathfrak{b}$, $\overline{\mathfrak{b}}$, $\mathfrak{c}$, $\overline{\mathfrak{c}}$ which proved useful is

$$\begin{aligned}
\mathfrak{b} &= \frac{\overline{l_1}+\overline{l_2}+\overline{l_3}+\overline{l_4}}{l_1+l_2+l_3+l_4}, \qquad \overline{\mathfrak{b}} = \frac{l_1+l_2+l_3+l_4}{\overline{l_1}+\overline{l_2}+\overline{l_3}+\overline{l_4}},\\
\mathfrak{c} &= \frac{l_1+l_2}{l_3+l_4}\cdot\frac{\overline{l_1}+\overline{l_2}+\overline{l_3}+\overline{l_4}}{l_1+l_2+l_3+l_4+\overline{l_1}+\overline{l_2}+\overline{l_3}+\overline{l_4}},\\
\overline{\mathfrak{c}} &= \frac{\overline{l_3}+\overline{l_4}}{\overline{l_1}+\overline{l_2}}\cdot\frac{l_1+l_2+l_3+l_4}{l_1+l_2+l_3+l_4+\overline{l_1}+\overline{l_2}+\overline{l_3}+\overline{l_4}},
\end{aligned} \tag{27}$$

where the functions l_j and $\overline{l_j}$ are closely related to the λ_j defined in (26)

$$\begin{aligned}
l_j(s) &= \lambda_j(s-i\gamma)\cdot\mathrm{e}^{\beta H}\phi^+(s)\phi^-(s),\\
\overline{l_j}(s) &= \lambda_j(s+i\gamma).
\end{aligned} \tag{28}$$

The main observation in connection with the functions defined in (27) is based on elementary facts of the theory of complex functions. In particular any analytic function on the complex plane is entirely determined by its singularities, i.e. poles and branch cuts, as well as its asymptotic behavior at infinity. Below we will show that the singularities of $\ln\mathfrak{b}$, $\ln\mathfrak{c}$ etc. on the *entire complex* plane are exhausted by the singularities of $\ln(1+\mathfrak{b})$, $\ln(1+\mathfrak{c})$ etc. close to the *real axis*[1]. Furthermore all the involved functions show constant asymptotics for N finite. Hence there exists a suitable integral representation of $\ln\mathfrak{b}$, $\ln\mathfrak{c}$ etc. in terms of $\ln(1+\mathfrak{b})$, $\ln(1+\mathfrak{c})$ etc. The latter functions will be abbreviated by

$$\begin{aligned}
\mathfrak{B} &= 1+\mathfrak{b} = \frac{l_1+l_2+l_3+l_4+\overline{l_1}+\overline{l_2}+\overline{l_3}+\overline{l_4}}{l_1+l_2+l_3+l_4},\\
\overline{\mathfrak{B}} &= 1+\overline{\mathfrak{b}} = \frac{l_1+l_2+l_3+l_4+\overline{l_1}+\overline{l_2}+\overline{l_3}+\overline{l_4}}{\overline{l_1}+\overline{l_2}+\overline{l_3}+\overline{l_4}},\\
\mathfrak{C} &= 1+\mathfrak{c} = \frac{l_1+l_2+l_3+l_4}{l_3+l_4}\cdot\frac{l_3+l_4+\overline{l_1}+\overline{l_2}+\overline{l_3}+\overline{l_4}}{l_1+l_2+l_3+l_4+\overline{l_1}+\overline{l_2}+\overline{l_3}+\overline{l_4}},\\
\overline{\mathfrak{C}} &= 1+\overline{\mathfrak{c}} = \frac{\overline{l_1}+\overline{l_2}+\overline{l_3}+\overline{l_4}}{\overline{l_1}+\overline{l_2}}\cdot\frac{l_1+l_2+l_3+l_4+\overline{l_1}+\overline{l_2}}{l_1+l_2+l_3+l_4+\overline{l_1}+\overline{l_2}+\overline{l_3}+\overline{l_4}}.
\end{aligned} \tag{29}$$

Quite generally all the above auxiliary functions have a product representation with factors of the type $\ldots+l_3+l_4+\overline{l_1}+\overline{l_2}+\ldots$. As a matter of the BAE the poles of each l_j and $\overline{l_j}$ function in $\ldots+l_3+l_4+\overline{l_1}+\overline{l_2}+\ldots$ are canceled by the neighboring terms. Poles can only "survive" if such a string does not begin with l_1 or does not end with $\overline{l_4}$. There are extended singularities (cuts) due to the function ϕ appearing in the definition of λ_1 and λ_4. Hence all terms $l_1+l_2+\ldots$ and $\ldots+\overline{l_3}+\overline{l_4}$ possess branch cuts along $[-1,1]+2i\gamma$ and $[-1,1]-2i\gamma$, respectively. Furthermore, terms like $\ldots+l_3+l_4$ and $\overline{l_1}+\overline{l_2}+\ldots$ have branch cuts along $[-1,1]$. However in combinations $\ldots+l_4+\overline{l_1}+\ldots$ the branch cut due to the ϕ function disappears, because

$$l_4(s)+\overline{l_1}(s) = \mathrm{e}^{\beta(\mu+H/2)}\frac{\phi^+(s)+\phi^-(s)}{q_1(s)}, \tag{30}$$

and $\phi^+(s)+\phi^-(s)$ is analytic everywhere.

Inspecting the function $\lambda_1+\lambda_2+\lambda_3+\lambda_4$ more closely we find poles of order $N/2$ at $s_0-i\gamma$ and $i\gamma-s_0$ where

$$z(s_0)=z_-(w), \qquad 2is_0\simeq N/\beta \text{ for large } N. \tag{31}$$

In addition we find zeros and branch cuts on the lines $\mathrm{Im}(s)=\pm\gamma$ which we denote by

$$\begin{aligned}
\ln[\lambda_1(s)+\lambda_2(s)+\lambda_3(s)+\lambda_4(s)] \equiv_s &-\frac{N}{2}\ln[(s+i\gamma-s_0)(s+s_0-i\gamma)]\\
&+L_-(s+i\gamma)+L_+(s-i\gamma),
\end{aligned} \tag{32}$$

[1]The relevant singularities are distributed exactly on the real axis for vanishing external fields. For this case the subsequent treatment can be taken literally. For finite external fields h, μ deviations from the real axis occur. The following reasoning still applies *mutatis mutandis*.

where $\equiv_s$ denotes that left and right hand sides have the same singularities on the entire plane, and $L_\pm$ are suitable functions possessing the desired singularities and being analytic otherwise. (The existence of such functions can be proved quite easily. An explicit expression is given by contour integrals of the type (37).) From (32) we find the following singularities

$$\begin{aligned}\ln[l_1(s)+l_2(s)+l_3(s)+l_4(s)] \equiv_s & -\frac{N}{2}\ln[(s-s_0)(s+s_0-2i\gamma)]+\ln[\phi^+(s)\phi^-(s)] \\ & + L_-(s)+L_+(s-2i\gamma), \\ \ln[\overline{l_1}(s)+\overline{l_2}(s)+\overline{l_3}(s)+\overline{l_4}(s)] \equiv_s & -\frac{N}{2}\ln[(s+2i\gamma-s_0)(s+s_0)] \\ & + L_-(s+2i\gamma)+L_+(s),\end{aligned} \tag{33}$$

From this, and (27,29) and the identity

$$\phi^+(s)\phi^-(s)=\left[\frac{(s-s_0)(s+s_0-2i\gamma)}{(s+s_0)(s-s_0+2i\gamma)}\right]^{N/2}, \tag{34}$$

we find the singularities

$$\begin{aligned}\ln \mathfrak{b}(s) &\equiv_s L_-(s+2i\gamma)+L_+(s)-L_-(s)-L_+(s-2i\gamma), \\ \ln \mathfrak{B}(s) &\equiv_s -L_-(s)+\text{rest}, \\ \ln \overline{\mathfrak{c}}(s)-\ln \overline{\mathfrak{C}}(s) &\equiv_s L_-(s)-L_+(s)+\text{rest},\end{aligned} \tag{35}$$

where "rest" indicates singularities not located on the real axis.

Next we introduce the notation

$$(g\circ f)(s)=\int_{\mathcal{L}} g(s-t)f(t)dt, \tag{36}$$

for the convolution of two functions g and f with contour $\mathcal{L}$ surrounding the real axis at infinitesimal distance above and below in anticlockwise manner. From Cauchy's theorem we find for any function f analytic above and below the real axis

$$(k\circ f)(x\pm i\epsilon)=(k\circ f)(x)+f(x\pm i\epsilon),\ \text{where } k(s)=\frac{1}{2\pi i}\frac{1}{s}. \tag{37}$$

For further convenience we introduce the functions

$$\begin{aligned}K_1(s)&=k(s)-k(s+2i\gamma)=\frac{\gamma/\pi}{s(s+2i\gamma)}, \\ \overline{K_1}(s)&=-k(s)+k(s-2i\gamma)=\frac{\gamma/\pi}{s(s-2i\gamma)}, \\ K_2(s)&=k(s-2i\gamma)-k(s+2i\gamma)=\frac{2\gamma/\pi}{s^2+4\gamma^2},\end{aligned} \tag{38}$$

which will play the role of integral kernels. From (35,37,38) we find

$$[K_2 \circ \ln \mathfrak{B} + \overline{K_1} \circ (\ln \overline{\mathfrak{c}} - \ln \overline{\mathfrak{C}})] \equiv_s L_-(s+2i\gamma) + L_+(s) - L_-(s) - L_+(s-2i\gamma). \quad (39)$$

Upon comparing (35,39) we conclude

$$\ln \mathfrak{b}(s) = K_2 \circ \ln \mathfrak{B} + \overline{K_1} \circ (\ln \overline{\mathfrak{c}} - \ln \overline{\mathfrak{C}}) + \text{const}, \quad (40)$$

as both sides are complex functions with identical singularities. (The difference function is entire, i.e. analytic on the entire complex plane. Furthermore the difference function is bounded, hence it is constant.) The constant is computed from considering the asymptotic behavior at $s \to \infty$

$$\text{const} = -\beta H. \quad (41)$$

For the derivation of the second type of integral equation we define an intermediate set of auxiliary functions

$$\begin{aligned} \tau &= \frac{l_1 + l_2}{l_3 + l_4}, \qquad T = 1 + \tau = \frac{l_1 + l_2 + l_3 + l_4}{l_3 + l_4}, \\ \overline{\tau} &= \frac{\overline{l_3} + \overline{l_4}}{\overline{l_1} + \overline{l_2}}, \qquad \overline{T} = 1 + \overline{\tau} = \frac{\overline{l_1} + \overline{l_2} + \overline{l_3} + \overline{l_4}}{\overline{l_1} + \overline{l_2}}. \end{aligned} \quad (42)$$

Quite similar to the above derivation we conclude the identity

$$\ln \tau(s) = \frac{N}{2} \ln \frac{s + s_0}{s + s_0 - 2i\gamma} + \beta(\mu + H/2) + \ln \phi(s) - \overline{K_1} \circ (\ln \overline{\mathfrak{B}} + \ln \overline{T}). \quad (43)$$

Next we deform the integration contour for $\ln \overline{\mathfrak{B}}$ in (43) from a narrow loop around the real axis to a wide loop consisting of the two horizontal lines $\text{Im} s = \pm\alpha$, with $0 < \alpha \leq \gamma$. The corresponding convolution is denoted by "$\square$"

$$\overline{K_1} \circ \ln \overline{\mathfrak{B}} = \overline{K_1} \square \ln \overline{\mathfrak{B}} - \ln \overline{\mathfrak{B}}, \quad (44)$$

and the additional contribution is due to the residue of $\overline{K_1}$. Taking into account of (27,42) we find

$$\ln \mathfrak{c} = \ln \tau - \ln \overline{\mathfrak{B}}, \qquad \Delta \ln \overline{T} = \Delta \ln \overline{\mathfrak{C}}, \quad (45)$$

where $\Delta f(x) = f(x + i0) - f(x - i0)$ denotes the discontinuity along the real axis. Therefore, (43) turns into

$$\ln \mathfrak{c}(s) = \frac{N}{2} \ln \frac{s + s_0}{s + s_0 - 2i\gamma} + \beta(\mu + H/2) + \ln \phi(s) - \overline{K_1} \square \ln \overline{\mathfrak{B}} - \overline{K_1} \circ \ln \overline{\mathfrak{C}}. \quad (46)$$

Lastly, we perform the limit $N \to \infty$ in the above equations yielding

$$\begin{aligned} \ln \mathfrak{b} &= -\beta H + K_2 \square \ln \mathfrak{B} + \overline{K_1} \circ (\ln \overline{\mathfrak{c}} - \ln \overline{\mathfrak{C}}), \\ \ln \mathfrak{c} &= -\beta U/2 + \beta(\mu + H/2) + \ln \phi - \overline{K_1} \square \ln \overline{\mathfrak{B}} - \overline{K_1} \circ \ln \overline{\mathfrak{C}}, \\ \ln \overline{\mathfrak{c}} &= -\beta U/2 - \beta(\mu + H/2) - \ln \phi + K_1 \square \ln \mathfrak{B} + K_1 \circ \ln \mathfrak{C}, \end{aligned} \quad (47)$$

where the equation for $\ln \overline{\mathfrak{c}}$ has been derived in analogy to the one for $\ln \mathfrak{c}$, and the function ϕ has the simplified expression

$$\ln \phi(x) = -2\beta i x \sqrt{1 - 1/x^2}. \tag{48}$$

We want to point out that the function $\mathfrak{b}$ will be evaluated on the lines $\mathrm{Im} s = \pm\alpha$. The functions $\mathfrak{c}$ and $\overline{\mathfrak{c}}$ need only be evaluated on the real axis infinitesimally above and below the interval $[-1, 1]$. Also the convolutions involving the "$\mathfrak{c}$ functions" in (47) can be restricted to a contour surrounding $[-1, 1]$ as these functions are analytic outside.

The detailed derivation of integral expressions for the largest eigenvalue Λ of the QTM is deferred to Appendix A. Here we restrict ourselves to a compilation of the most relevant results

$$\begin{aligned}
2\pi i \ln \Lambda =& 2\pi i\beta(\mu + U/4) + \int_{\mathcal{L}} [\ln z(s)]' \ln\left(1 + \mathfrak{c} + \overline{\mathfrak{c}}\right) ds \\
&- \frac{1}{2}\int_{\mathcal{L}} \left[\ln \frac{z(s - 2i\gamma)}{z(s)}\right]' \ln \mathfrak{B}(s) ds - \frac{1}{2}\int_{\mathcal{L}} \left[\ln \frac{z(s + 2i\gamma)}{z(s)}\right]' \ln \overline{\mathfrak{B}}(s) ds, \\
=& 2\pi i\beta(\mu + H/2 + U/4) + \int_{\mathcal{L}} [\ln z(s)]' \ln\left(1 + \mathfrak{c} + \overline{\mathfrak{c}}\right) ds \\
&- \int_{\mathcal{L}} \left[\ln \frac{z(s - 2i\gamma)}{z(s)}\right]' \ln \mathfrak{B}(s) ds, \\
=& -2\pi i\beta \frac{U}{4} + \int_{\mathcal{L}} [\ln z(s)]' \ln \frac{1 + \mathfrak{c} + \overline{\mathfrak{c}}}{\overline{\mathfrak{c}}} ds + \int_{\mathcal{L}} [\ln z(s - 2i\gamma)]' \ln \mathfrak{C}(s) ds.
\end{aligned} \tag{49}$$

The last two expressions are of particular importance to our further numerical and analytical treatment.

Finally, we want to comment on the structure of the equations determining the thermodynamical properties of the Hubbard model. In contrast to long-range interaction systems [46, 47] we have to solve a set of subsidiary equations (47) for the "distribution functions" $\mathfrak{b}$, $\mathfrak{c}$, and $\overline{\mathfrak{c}}$ before evaluating the free energy (49). Obviously, the dynamics of the elementary excitations of the nearest-neighbor systems is more involved than those of [46, 47] which may be viewed as "free particles with exclusion statistics".

6 Numerical Results

For the numerical treatment of equations (47,49) we rewrite them in terms of usual convolutions of functions of a real variable

$$K * f = \int_{-\infty}^{\infty} K(x - y)\, f(y)\, \mathrm{d}y. \tag{50}$$

For the functions (27) evaluated on the contours involved in (47,49) we use the notation $\mathfrak{b}^{\pm}$, $\mathfrak{c}^{\pm}$ and $\overline{\mathfrak{c}^{\pm}}$

$$\mathfrak{b}^{\pm}(x) = \mathfrak{b}(x \pm i\alpha), \quad \mathfrak{c}^{\pm}(x) = \mathfrak{c}(x \pm i\,0), \quad \overline{\mathfrak{c}^{\pm}}(x) = \overline{\mathfrak{c}}(x \pm i\,0), \tag{51}$$

where the shift α in $\mathfrak{b}$ is arbitrary but fixed with $0 < \alpha \leq \gamma$. (For many numerical calculation we take $\alpha = 2\gamma/3$ and especially $\alpha = \gamma$.) Furthermore, we introduce the following relations:

$$\begin{aligned} \mathfrak{B}^{\pm} &:= 1 + \mathfrak{b}^{\pm}, & \overline{\mathfrak{B}^{\pm}} &:= 1 + 1/\mathfrak{b}^{\pm}, \\ \mathfrak{C}^{\pm} &:= 1 + \mathfrak{c}^{\pm}, & \overline{\mathfrak{C}^{\pm}} &:= 1 + \overline{\mathfrak{c}^{\pm}}, \\ \Delta \log \mathfrak{C} &:= \log(\mathfrak{C}^{+}/\mathfrak{C}^{-}), & \Delta \log \overline{\mathfrak{C}} &:= \log(\overline{\mathfrak{C}^{+}}/\overline{\mathfrak{C}^{-}}). \end{aligned} \tag{52}$$

Thus (47) is written in the form

$$\begin{aligned} \log \mathfrak{b}^{\pm} &= -\beta H - K_{2,\pm\alpha-\alpha} * \log \mathfrak{B}^{+} + K_{2,\pm\alpha+\alpha} * \log \mathfrak{B}^{-} - \overline{K}_{1,\pm\alpha} * \Delta \log(\overline{\mathfrak{r}}/\overline{\mathfrak{C}}), \\ \log \mathfrak{c}^{\pm} &= \Psi_{\mathfrak{c}}^{\pm} + \overline{K}_{1,-\alpha} * \log \overline{\mathfrak{B}^{+}} - \overline{K}_{1,\alpha} * \log \overline{\mathfrak{B}^{-}} + \overline{K}_{1,0} * \Delta \log \overline{\mathfrak{C}} \pm \tfrac{1}{2} \Delta \log \overline{\mathfrak{C}}, \\ \log \overline{\mathfrak{c}^{\pm}} &= \overline{\Psi}_{\mathfrak{c}}^{\pm} - K_{1,-\alpha} * \log \mathfrak{B}^{+} + K_{1,\alpha} * \log \mathfrak{B}^{-} - K_{1,0} * \Delta \log \mathfrak{C} \pm \tfrac{1}{2} \Delta \log \mathfrak{C}, \end{aligned} \tag{53}$$

where

$$\Psi_{\mathfrak{c}}^{\pm} = -\beta U/2 + \beta(\mu + H/2) + \log \phi_{\pm 0}, \tag{54}$$

$$\overline{\Psi}_{\mathfrak{c}}^{\pm} = -\beta U/2 - \beta(\mu + H/2) - \log \phi_{\pm 0}, \tag{55}$$

and we have used the notation f_α for a function f with shift of the argument by $i\alpha$

$$f_\alpha(x) = f(x + i\alpha).$$

In particular $\phi_{\pm 0}$ denotes the function ϕ evaluated on the real axis from above/below. Notice that the convolution over the terms $\Delta \log \mathfrak{C}$ and $\Delta \log \overline{\mathfrak{C}}$ are determined by Cauchy's principal value. Remember that these functions vanish outside the interval $[-1, 1]$.

Similarly, from (49) we obtain two different relations for the eigenvalue

$$\begin{aligned} \log \Lambda &= -\int_{-1}^{1} \mathcal{K} \, \log[(1 + \mathfrak{c}^{+} + \overline{\mathfrak{c}^{+}})(1 + \mathfrak{c}^{-} + \overline{\mathfrak{c}^{-}})] \, \mathrm{d}x \\ &\quad + \int_{-\infty}^{\infty} [(\mathcal{K}_{\alpha-2\gamma} - \mathcal{K}_{\alpha}) \, \log \mathfrak{B}^{+} \, - \, (\mathcal{K}_{-\alpha-2\gamma} - \mathcal{K}_{-\alpha}) \, \log \mathfrak{B}^{-}] \, \mathrm{d}x \, + \beta(\mu + H/2 + U/4). \\ &= -\int_{-1}^{1} \mathcal{K} \, \log[(1 + \mathfrak{c}^{+} + \overline{\mathfrak{c}^{+}})(1 + \mathfrak{c}^{-} + \overline{\mathfrak{c}^{-}})/(\overline{\mathfrak{c}^{+}} \, \overline{\mathfrak{c}^{-}})] \, \mathrm{d}x \\ &\quad - \int_{-1}^{1} \mathcal{K}_{-2\gamma} \, \log[(1 + \mathfrak{c}^{+})/(1 + \mathfrak{c}^{-})] \, \mathrm{d}x \, - \beta U/4, \end{aligned} \tag{56}$$

with

$$\mathcal{K}(x) = -\left(2\pi\sqrt{1 - x^2}\right)^{-1} = \left(2\pi i \, x\sqrt{1 - 1/x^2}\right)^{-1}, \tag{57}$$

and $\mathcal{K}_\alpha$ is the related function with shifted argument. The branch of $\mathcal{K}$ is fixed by the requirement $\mathcal{K}(x) \simeq 1/(2\pi i x)$ for large x. By means of the relation

$$\Delta \log \overline{\mathfrak{r}} = -\Delta \log \phi + \Delta \log \mathfrak{C},$$

the first equation of (53) turns into

$$\log \mathfrak{b}^{\pm} = \Psi_{\mathfrak{b}}^{\pm} - K_{2,\pm\alpha-\alpha} * \log \mathfrak{B}^{+} + K_{2,\pm\alpha+\alpha} * \log \mathfrak{B}^{-} - \overline{K}_{1,\pm\alpha} * \Delta \log(\mathfrak{C}/\overline{\mathfrak{C}}), \tag{58}$$

where

$$\Psi_{\mathfrak{b}}^{\pm} = -\beta U - \beta H + \log \phi_{\pm\alpha} - \log \phi_{\pm\alpha-2\gamma}. \tag{59}$$

For the sake of completeness rather than for further applications we mention the results for finite Trotter number N. All equations above hold true after the replacement of the "driving functions" ψ by

$$\begin{aligned}
\Psi_{\mathfrak{b}}^{\pm} &= -\beta H + \log \phi_{\pm\alpha} - \log \phi_{\pm\alpha-2\gamma} - \tfrac{N}{2} \log \tfrac{x \pm i\alpha - s_0 + 2i\gamma}{x \pm i\alpha - s_0 - 2i\gamma}, \\
\Psi_{\mathfrak{c}}^{\pm} &= +\beta(\mu + H/2) + \log \phi_{\pm 0} + \tfrac{N}{2} \log \tfrac{x + s_0}{x + s_0 - 2i\gamma}, \\
\overline{\Psi}_{\mathfrak{c}}^{\pm} &= -\beta(\mu + H/2) - \log \phi_{\pm 0} + \tfrac{N}{2} \log \tfrac{x - s_0}{x - s_0 + 2i\gamma},
\end{aligned}$$

where s_0 is defined in (31). These relations for finite Trotter number N have been used for a comparison of the results of the integral equations with a direct treatment based on the BAE of Sections 3 and 4. Thus it was possible to ensure the accuracy (10^{-6}) of our numerics based on iterations and fast Fourier transform.

Next we present our numerical results for various physical quantities and discuss them in terms of the elementary spin and charge excitations, i.e. "spinons" and "holons" (plus gapped excitations based on "doubly occupied sites"). Note that at half-filling the system possesses a charge gap such that the holons do not contribute at low temperatures. Furthermore, the hopping integral of the kinetic energy has been set to $t = 1$.

In Fig.3 the temperature dependence of the specific heat is shown for densities $n = 1$, 0.8, and 0.5. For half-filling ($n = 1.0$) the specific heat shows one pronounced temperature maximum for lower values of the interaction U. For stronger U this maximum splits into a lower and a higher temperature maximum which are due to spin and (gapped) charge excitations, respectively. (These findings agree largely with those of [48].) The picture remains qualitatively true for small dopings ($n = 0.8$), however now the lower temperature peak receives contributions by gapless charge excitations, hence some weight is shifted from higher to lower temperatures. The situation changes quite drastically for fillings $n \approx 0.5$. Here a pronounced maximum in the specific heat is located at a temperature of about $T \approx 0.6$ which seems rather insensitive to the interaction. This is explained by the irrelevance of the onsite interaction at sufficiently large temperatures, because of the low particle density. In addition, we find a maximum at very low temperatures which depends very sensitively on U as well as on the particle density n. In order to clarify the origin of this additional structure the variation of the specific heat with n is shown in Fig.4 for $U = 8$. Decreasing the particle density n from half-filling ($n = 1$) to lower values ($n \approx 0.8$) the "spin" maximum at lower temperature increases. This picture is changed drastically below $n \lesssim 0.8$. Here the "spin" maximum and its location are suppressed for lower n and a shoulder at a higher temperature develops into a clear maximum. This new structure in the specific heat is located at about $T \approx 0.6$ and quite independent of U

as already mentioned. We interpret this maximum to be of "charge" type. The complex behavior at intermediate densities $0.5 \lesssim n \lesssim 0.7$ is due to a crossover of the "spin" and "charge" maxima, see also Fig.9. For densities $n \approx 1$ the "spin" maximum is located at finite temperature with finite height whereas the "charge" maximum is located at very small temperature with small height. For densities close to $n \approx 0$ the situation is reversed.

In Fig.5 and Fig.6 the magnetic susceptibility χ is presented. Again we begin our discussion with the half-filled case which is known to correspond to the Heisenberg spin chain with interaction strength of order $O(t^2/U)$. In fact, we observe a Heisenberg-like temperature dependence of the susceptibility with $\chi_{\max}$ and $T_{\max}$ scaling with U and $1/U$ in the range of $U = 4, ..., 8$. Upon doping this behavior remains qualitatively and quantitatively unchanged even for $n = 0.5$. Quite generally, the location $T_{\max}$ is shifted to lower temperatures, see Fig.6. The maximal value $\chi_{\max}$ decreases for decreasing particle density from $n = 1$ to $n \approx 0.8$. Below the value $n \lesssim 0.8$ the maximum $\chi_{\max}$ increases for further lowering of the particle density. This behavior is qualitatively explained by partially filled bands of charge carriers with spin.

In contrast to χ the charge susceptibility κ ($=\partial n/\partial\mu$, i.e. compressibility) shows a more interesting dependence on the particle density n, see Fig.7 and Fig.8. At half-filling κ shows the expected exponentially activated form with vanishing zero temperature value due to the charge gap. For any doping the low-temperature behavior is changed completely with finite value at zero temperature consistent with a partial filling of the lower Hubbard band. For density $n = 0.5$ we observe two different structures at low temperature similar to the case of the specific heat. The lower temperature "spin" peak resembles the structure in the susceptibility χ, whereas the "charge" maximum at slightly higher temperature is caused by the single particle motion of the bare electrons. The compressibility has a singular dependence on doping. The smaller the doping the closer the curves are at high temperatures and *the more divergent* at lower temperature, see Fig.8. This, of course, is exactly the behavior of a system exhibiting a Mott-Hubbard transition at half-filling.

Our findings are qualitatively in accordance with the results[2] of [17, 18] for the dopings treated therein. In particular for specific heats, magnetic and charge susceptibilities the results compare well for densities $0.7 \leq n \leq 1$ and temperatures $T \geq 0.1$, giving an independent support to the truncation approximation adopted there.

The present approach has the advantage of explicit evaluations over much wider temperature and density regions. The T-linearity of the specific heat at very low temperatures, as expected from CFT, is clearly observed in contrast to [18]. Moreover, we have novel observations of additional structures at lower temperatures and densities especially in the compressibility as mentioned above. These structures can be also interpreted in terms of CFT and zero temperature excitations. Therefore, we conclude that the present approach is the first one making possible the explicit evaluation of the crossover from the very low temperature (CFT) to the very high temperature region in an exact way.

In Fig.9 we show a separation of the specific heat into spin and charge components. This is done in principle on the basis of eigenvalue equations like (56). As motivated by

[2] In [17, 18] notice the factor 4 for the interaction U.

the study of the strong-coupling limit in section 7.1, contributions by $\mathfrak{b}$ and $\mathfrak{c}$ functions are interpreted as spin and charge contributions, respectively. However, the procedure is not unique as we have various alternative formulations resulting in different separations. In particular we like to note the expression

$$\begin{aligned}\ln\Lambda = -\beta(e_0 - U/4 - \mu) \;\; &+ \;\; \int_{-1}^{1} \left[c_0 \Delta \ln \mathfrak{C}/\overline{\mathfrak{C}} - \mathcal{K} \ln(1+\mathfrak{c}^+ + \overline{\mathfrak{c}}^+)(1+\mathfrak{c}^- + \overline{\mathfrak{c}}^-)\right] dx \\ &+ \;\; \int_{-\infty}^{\infty} c_2(x) \ln \mathfrak{B}^-(x) dx + \int_{-\infty}^{\infty} c_1(x) \ln \overline{\mathfrak{B}}^+(x) dx, \qquad (60)\end{aligned}$$

with

$$c_0(x) = \frac{1}{2\pi}\int_{-\infty}^{\infty} \frac{J_0(k)}{1+e^{U|k|/2}} e^{ikx} dk, \qquad c_{1,2}(x) = \frac{1}{2\pi}\int_{-\infty}^{\infty} \frac{J_0(k)}{1+e^{\mp Uk/2}} e^{ikx} dk. \qquad (61)$$

Here e_0 is the groundstate energy at half-filling as given in [1] and the additional contributions by $\mathfrak{b}$ and $\mathfrak{c}$ functions represent correction terms due to spin and charge excitations. In Fig.9 we show the results for the specific heat

$$c = T\left(\frac{\partial S}{\partial T}\right)_{\mu} + T\left(\frac{\partial n}{\partial T}\right)_{\mu}\left(\frac{\partial \mu}{\partial T}\right)_{n}, \qquad (62)$$

where we have applied the separation based on (60) to the temperature derivatives of S and n. Note the functional form of the spin part which is rather independent of the doping. However, upon small doping the charge contribution develops a low-temperature peak which disappears again for larger dopings. We would like to comment on the issue of the "mathematical separation" of spin and charge as described above (and similarly applied in [17, 18]) that it may give rise to artificial results. For instance, at higher temperatures the "partial specific heats" show negative values whereas the total specific heat is always positive. In section 7.3 the spin-charge separation is treated at low temperatures and arbitrary particle density via an involved interplay of the various degrees of freedom rather than by a superficial interpretation of formulas.

7 Analytical solutions of the integral equations

In the previous sections we have derived non-linear integral equations for the largest eigenvalue being directly related to the free energy of the Hubbard model at finite temperatures $T = 1/\beta$. For arbitrary temperatures and densities the integral equations can be solved only numerically. However, in some limiting cases analytical results can be derived and relations obtained which permit a comparison to known analytical results. This implies the consistency of our approach.

7.1 Strong-coupling limit

In the strong-coupling limit $U \to \infty$ at half-filling ($\mu = 0$) the Hubbard model is expected to reduce to the Heisenberg chain. Indeed, in the strong-coupling limit we find directly the thermodynamics of the Heisenberg model. This can be seen as follows:

Considering the limit $\gamma \to \infty$ (with $\gamma = U/4$) we rescale the argument of the auxiliary functions by $x \mapsto 2\gamma x$ as well as the ratio $\beta/(2\gamma) \mapsto \tilde{\beta}$ and $(2\gamma)H \mapsto \tilde{H}$. It turns out that all contributions of $\mathfrak{c}^{\pm}$ and $\overline{\mathfrak{c}^{\pm}}$ can be dropped in (58) because of their vanishing range of integration. Moreover $\mathfrak{c}^{\pm}$ and $\overline{\mathfrak{c}^{\pm}}$ tend to zero. The remaining equations read

$$\log \mathfrak{b}^{\pm} = \Psi^{\pm}_{\mathfrak{b}} - K_{2,\pm\alpha-\alpha} * \log \mathfrak{B}^{+} + K_{2,\pm\alpha+\alpha} * \log \mathfrak{B}^{-} \quad \text{with} \quad \Psi^{\pm}_{\mathfrak{b}} = -\tilde{\beta}\tilde{H} + 2\pi\tilde{\beta}\,\overline{K}_{1,\pm\alpha}. \tag{63}$$

According to equation (56) and after dropping the groundstate energy shift $\beta U/4$ the eigenvalue is

$$\log \Lambda = K_{1,-\alpha} * \log \mathfrak{B}^{+}|_{x=0} - K_{1,\alpha} * \log \mathfrak{B}^{-}|_{x=0} + \tilde{\beta}\tilde{H}/2. \tag{64}$$

Now we define

$$b := 1/\mathfrak{b}^{+}, \quad B := 1 + b \quad \text{and} \quad \overline{b} := \mathfrak{b}^{-}, \quad \overline{B} := \mathfrak{B}^{-}, \tag{65}$$

which are inserted into the integral equations. By means of the identity

$$\log \mathfrak{B}^{+} = \log B - \log b,$$

we have

$$\begin{aligned} -\log b - K_{2,0} * \log b &= +\Psi^{+}_{\mathfrak{b}} - K_{2,0} * \log B + K_{2,2\alpha} * \log \overline{B}, \\ -\log \overline{b} - K_{2,0} * \log \overline{b} &= -\Psi^{-}_{\mathfrak{b}} + K_{2,-2\alpha} * \log B - K_{2,0} * \log \overline{B}. \end{aligned}$$

Using the Fourier transform this provides

$$\log b = +\tilde{\beta}\tilde{H}/2 - 2\pi\tilde{\beta}\,\Phi_{+\alpha} + R_0 * \log B - R_{+2\alpha} * \log \overline{B}, \tag{66}$$

$$\log \overline{b} = -\tilde{\beta}\tilde{H}/2 - 2\pi\tilde{\beta}\,\Phi_{-\alpha} + R_0 * \log \overline{B} - R_{-2\alpha} * \log B, \tag{67}$$

with the eigenvalue

$$\log \Lambda = 2\tilde{\beta}\log 2 + \int_{-\infty}^{\infty} \big(\Phi_{\alpha} \log B - \Phi_{-\alpha} \log \overline{B} \big)\, \mathrm{d}x, \tag{68}$$

and

$$\Phi_{\alpha} = \frac{i}{2\sinh \pi(x + i\alpha)}, \quad R_{\alpha} = \int_{-\infty}^{\infty} \frac{\mathrm{d}k}{2\pi}\, \frac{\mathrm{e}^{ikx - k\alpha}}{1 + \mathrm{e}^{|k|}}.$$

These relations correspond to the non-linear integral equations of the isotropic antiferromagnetic spin-1/2 Heisenberg chain [25, 26]. In addition, this case is also related to the thermodynamics of the $t - J$ model at half-filling [30].

7.2 Free-Fermion limit

Let us consider the opposite limit $U \to 0$ (at $\mu = 0$ and $H = 0$), that is, the case of two independent Free-Fermion systems. The non-linear integral equations (53) simplify to an algebraic set of equations

$$\begin{aligned}
\log \mathfrak{b}^{\pm} &= -\beta H - \log \mathfrak{B}^{+} + \log \mathfrak{B}^{-} - (\tfrac{1}{2} \pm \tfrac{1}{2})\, \Delta \log(\overline{\mathfrak{c}}/\overline{\mathfrak{C}}), \\
\log \mathfrak{c}^{\pm} &= +\beta(\mu + H/2) + \log \phi_{\pm} - \log \overline{\mathfrak{B}}^{-} + (\tfrac{1}{2} \pm \tfrac{1}{2})\, \Delta \log \overline{\mathfrak{C}}, \\
\log \overline{\mathfrak{c}^{\pm}} &= -\beta(\mu + H/2) - \log \phi_{\pm} - \log \mathfrak{B}^{+} + (-\tfrac{1}{2} \pm \tfrac{1}{2})\, \Delta \log \mathfrak{C},
\end{aligned}$$

with

$$\log \Lambda = -\int_{-1}^{1} \mathcal{K}_0 \, \log \frac{(1 + \mathfrak{c}^{+} + \overline{\mathfrak{c}^{+}})(1 + \mathfrak{c}^{-} + \overline{\mathfrak{c}^{-}})(1 + \mathfrak{c}^{-})}{\overline{\mathfrak{c}^{+}}\, \overline{\mathfrak{c}^{-}}\, (1 + \mathfrak{c}^{+})} \, \mathrm{d}x.$$

The solution reads as follows

$$\begin{aligned}
\mathfrak{b}^{+} &= \frac{\left[1 + \mathrm{e}^{\beta(\mu + H/2)} \phi\right] \left[1 + \mathrm{e}^{\beta(\mu - H/2)}/\phi\right]}{\mathrm{e}^{\beta H} \left[\mathrm{e}^{\beta(\mu + H/2)}/\phi + \mathrm{e}^{2\beta\mu} + 1 + \mathrm{e}^{\beta(\mu - H/2)}/\phi\right]}, \\
\mathfrak{b}^{-} &= \frac{\left[\mathrm{e}^{\beta(\mu + H/2)}/\phi + \mathrm{e}^{2\beta\mu} + 1 + \mathrm{e}^{\beta(\mu - H/2)}/\phi\right]}{\mathrm{e}^{\beta H} \left[1 + \mathrm{e}^{\beta(\mu + H/2)}/\phi\right] \left[1 + \mathrm{e}^{\beta(\mu - H/2)} \phi\right]}, \\
\mathfrak{c}^{+} &= \frac{\mathrm{e}^{\beta(\mu + H/2)}}{\phi} \frac{1 + \mathrm{e}^{\beta(\mu - H/2)} \phi}{1 + \mathrm{e}^{\beta(\mu - H/2)}/\phi} \frac{\mathfrak{b}^{+}}{1 + \mathfrak{b}^{+}}, \qquad \mathfrak{c}^{-} = \frac{\mathrm{e}^{\beta(\mu + H/2)}}{\phi} \frac{\mathfrak{b}^{-}}{1 + \mathfrak{b}^{-}}, \\
\overline{\mathfrak{c}}^{+} &= \frac{1}{\mathrm{e}^{\beta(\mu + H/2)} \phi (1 + \mathfrak{b}^{+})}, \qquad \overline{\mathfrak{c}}^{-} = \frac{\phi}{\mathrm{e}^{\beta(\mu + H/2)}} \frac{1 + \mathrm{e}^{\beta(\mu - H/2)}/\phi}{1 + \mathrm{e}^{\beta(\mu - H/2)} \phi} \frac{1}{1 + \mathfrak{b}^{-}},
\end{aligned}$$

Lastly, we substitute $x = \sin k$ in the integration for the eigenvalue which leads to

$$\begin{aligned}
\log \Lambda = &+ \frac{1}{2\pi} \int_{-\pi}^{\pi} \ln \left[1 + \exp\left(\beta(\mu + H/2 + 2\cos k)\right)\right] \mathrm{d}k \\
&+ \frac{1}{2\pi} \int_{-\pi}^{\pi} \ln \left[1 + \exp\left(\beta(\mu - H/2 + 2\cos k)\right)\right] \mathrm{d}k.
\end{aligned}$$

This is the desired result.

7.3 Low-temperature asymptotics

The low-temperature regime is the most interesting limit as the system shows Tomonaga-Luttinger liquid behavior. We will derive analytic expressions for the thermodynamics within our first principles calculations and confirm the field theoretical predictions. In particular we will show how the non-linear integral equations correspond to the known dressed energy formalism of the Hubbard model. This represents a further and in fact the most interesting consistency check.

For $T = 1/\beta \ll 0$ we can simplify the non-linear integral equations as follows. We adopt fields $H > 0$, $\mu < 0$, such that $\mathfrak{b}^- \to 0$, $\mathfrak{c}^\pm \to 0$ and $1/\overline{\mathfrak{c}}^- \to 0$ at $\beta \gg 1$ which can be verified numerically. Moreover, one finds

$$|\mathfrak{b}^+|,\, |1/\overline{\mathfrak{c}}^+| \gg 1 \quad \text{for} \quad |x| < \lambda_0,\, \sigma_0 \quad \text{and} \quad |\mathfrak{b}^+|,\, |1/\overline{\mathfrak{c}}^+| \ll 1 \quad \text{for} \quad |x| > \lambda_0,\, \sigma_0,$$

for certain crossover values λ_0, σ_0. The slopes for the crossover are steep, so that the following approximations to the integral equations (53) are valid:

$$\begin{aligned}
\log \mathfrak{b}^+ &= \phi_b - \int_{-\lambda_0}^{+\lambda_0} K_2(\lambda - \lambda')\, \log \mathfrak{b}^+(\lambda')\, \mathrm{d}\lambda' + \int_{-k_0}^{+k_0} \overline{K}_{1,\alpha}(\lambda - \sin k')\, \cos k'\, \log \mathfrak{c}^\vee(k')\, \mathrm{d}k' \\
\log \mathfrak{c}^\vee &= \phi_c + \int_{-\lambda_0}^{+\lambda_0} K_{1,-\alpha}(\sin k - \lambda')\, \log \mathfrak{b}^+(\lambda')\, \mathrm{d}\lambda'.
\end{aligned} \tag{69}$$

Here we use $\mathfrak{c}^\vee(k) = 1/\overline{\mathfrak{c}}^+(\sin k)$ and $\sigma_0 = \sin k_0$. The driving terms read

$$\begin{aligned}
\phi_b(\lambda) &= -\beta\varepsilon_s^0(\lambda) - \frac{\pi^2(K_2(\lambda - \lambda_0) + K_2(\lambda + \lambda_0))}{6(\log 1/\mathfrak{b}^+)'(\lambda_0)} \\
&\qquad + \frac{\pi^2 \cos k_0 (K_{1,\alpha}(\lambda - \sin k_0) + K_{1,\alpha}(\lambda + \sin k_0))}{6(\log 1/\mathfrak{c}^\vee)'(k_0)}, \\
\phi_c(\lambda) &= -\beta\varepsilon_c^0(\lambda) + \frac{\pi^2(K_{1,-\alpha}(\sin k - \lambda_0) + K_{1,-\alpha}(\sin k + \lambda_0))}{6(\log 1/\mathfrak{b}^+)'(\lambda_0)},
\end{aligned} \tag{70}$$

where $\varepsilon_s^0 = H$, $\varepsilon_c^0 = -\mu - U/2 - H/2 - 2\cos k$. Retaining only the leading terms in the integral equations and choosing the imaginary part of the integration contour as $\alpha = \gamma$, we find the following connections between auxiliary functions and the dressed energy functions:

$$\log \mathfrak{b}^+ = -\beta\, \varepsilon_s + O(1/\beta) \quad \text{and} \quad \log \mathfrak{c}^\vee = -\beta\, \varepsilon_c + O(1/\beta). \tag{71}$$

For a comparison with [12, 13] note the different normalization of the chemical potential. The free energy also admits the same approximation scheme yielding up to $O(T^2)$ terms in the low-temperature expansion. To present this, we introduce "root density functions" ρ by the definition

$$\begin{aligned}
\rho_s(\lambda) &= -\int_{-\lambda_0}^{+\lambda_0} K_2(\lambda - \lambda')\, \rho_s(\lambda')\, \mathrm{d}\lambda' + \int_{-k_0}^{+k_0} \overline{K}_{1,\alpha}(\lambda - \sin k')\, \rho_c(k')\, \mathrm{d}k' \\
\rho_c(k) &= \frac{1}{2\pi} + \cos k \int_{-\lambda_0}^{+\lambda_0} K_{1,-\alpha}(\sin k - \lambda')\, \rho_s(\lambda')\, \mathrm{d}\lambda'.
\end{aligned} \tag{72}$$

Note that the kernel matrices for the integral equations (69, 72) are mutually transpose. The following equality is an immediate consequence:

$$\frac{1}{2\pi}\int_{-k_0}^{+k_0}\log\mathfrak{c}^{\vee}(k)\mathrm{d}k=\int_{-k_0}^{+k_0}\rho_c(k)\,\phi_c(k)\,\mathrm{d}k+\int_{-\lambda_0}^{+\lambda_0}\rho_s(\lambda)\,\phi_b(\lambda)\,\mathrm{d}\lambda. \tag{73}$$

With these relations the eigenvalue ($\log\Lambda$) reads

$$\log\Lambda=-\beta\gamma+\int_{-k_0}^{+k_0}\rho_c(k)\,\phi_c(k)\,\mathrm{d}k+\int_{-\lambda_0}^{+\lambda_0}\rho_s(\lambda)\,\phi_b(\lambda)\,\mathrm{d}\lambda+\frac{\pi}{6\beta\varepsilon_c'(k_0)}, \tag{74}$$

where we have replaced $(\log 1/\mathfrak{c}^{\vee})'(k_0)$ in the denominator by $\beta\varepsilon_c'(k_0)$. Substituting (70) into (74) we arrive at the final expression,

$$f=\varepsilon_0-\frac{\pi}{6\beta^2}\left(\frac{1}{v_c}+\frac{1}{v_s}\right). \tag{75}$$

The definitions of sound velocity and the ground state energy coincide with standard results, $v_{s,c}=\varepsilon_{s,c}'/2\pi\rho_{s,c}|_{\lambda_0,k_0}$, and

$$\varepsilon_0=\int_{-k_0}^{+k_0}\rho_c(k)\,\epsilon_c^0(k)\,\mathrm{d}k+\int_{-\lambda_0}^{+\lambda_0}\rho_s(\lambda)\,\epsilon_s^0(\lambda)\,\mathrm{d}\lambda.$$

Here the trivial shift in the energy $U/4$ is omitted. We thereby conclude that our formalism completely recovers the correct contribution from spinon and holon excitations in the low temperature behavior. This is a manifestation of spin-charge separation due to which each elementary excitation contributes independently to (75) where the velocities v_c and v_s typically take different values.

7.4 High-temperature limit

Finally, we consider the high-temperature limit $T\to\infty$ with H,U as well as $\beta\mu$ fixed. The auxiliary functions in (58) become constant

$$\begin{aligned}&\log\mathfrak{b}^{\pm}=0,\quad \log\mathfrak{c}^{\pm}=\beta\mu-\log 2,\quad \log\overline{\mathfrak{c}^{\pm}}=-\beta\mu-\log 2,\\ \hookrightarrow\quad &\log\Lambda=\log(1+\mathfrak{c}+\overline{\mathfrak{c}})/\overline{\mathfrak{c}}.\end{aligned}$$

Thus, the free energy reads

$$f=-2\,T\log(1+\mathrm{e}^{\mu/T})\quad\text{with}\quad \mu/T=\log\frac{n}{2-n}, \tag{76}$$

where n is the particle density. We obtain the entropy

$$S=2\log\frac{2}{2-n}-n\log\frac{n}{2-n}, \tag{77}$$

as expected by counting the degrees of freedom per lattice site. Especially, at half-filling $n=1$ this equals to $S=\log(4)$.

8 Summary and Discussion

In this paper, the novel formulation of thermodynamics for 1D quantum systems has been successfully applied to the Hubbard model. Several quantities of physical interests have been evaluated with high numerical precision and various limiting cases have been studied analytically.

As already noted above, we may consider as one of the most practical advantages of the present formulation the fact that one only has to deal with a finite number of unknown functions and nonlinear integral equations among them. This does not only imply convenience, rather it opens a more fundamental understanding related to the particle picture of 1D quantum systems. For the Heisenberg model, the complex conjugate auxiliary functions play a role which seems to correspond to the elementary spinon excitations [49, 50, 51], while for the integrable $t-J$ model one further function related to the holon is needed. In this paper, we have shown that three independent functions $\mathfrak{b}, \mathfrak{c}, \overline{\mathfrak{c}}$ describe the complete thermodynamics, physically corresponding to spinons, and holons in upper and lower Hubbard bands. In the $T \to 0$ limit, these functions are shown to reduce to energy density functions ("dressed energy functions") for such elementary excitations.

This interpretation which is natural at low temperatures poses however a problem at finite temperatures. The auxiliary functions, related to energies of excitations at $T = 0$, are no longer real for arbitrary temperature. Thus they lose the direct connection to physical excitations in the sense of energy levels. On the other hand, imaginary parts of energies indicate a finite life-time of excitations, or in this case a decay of the elementary particles of the system. We leave the investigation of these questions as an interesting future problem.

Obviously, our formulation can be extended to the evaluation of the asymptotics of correlation functions, such as spin-spin correlation lengths etc. These investigations on highly correlated electron systems, including the Hubbard, the integrable $t-J$, supersymmetric U models will be reported together in the near future.

Acknowledgements

The authors acknowledge financial support by the *Deutsche Forschungsgemeinschaft* under grant No. Kl 645/3-1 and support by the research program of the Sonderforschungsbereich 341, Köln-Aachen-Jülich.

A Derivation of integral expressions for the eigenvalue

Here we turn to the derivation of expressions for the largest eigenvalue of the QTM in terms of the above auxiliary functions. We calculate $\sum_j \ln z_j$ by a Cauchy integral of the function $f(s) = \ln z(s) \left[\ln\left(1 + l_4/l_3(s)\right)\right]'$ where the zeros of $(1 + l_4/l_3(s))$ in the neighborhood of the real axis are precisely the s_j. Furthermore we use a contour $\mathcal{L}_0$ surrounding the s_j in anticlockwise manner. The s_j are not located on the branch cut of $\ln z(s)$ from -1 to 1, hence $\mathcal{L}_0$ consists of two disconnected parts. (For not too low temperatures and vanishing external fields these parts are loops around $]-\infty, -1]$ and $[1, \infty[$, respectively. In the general case they are appropriately deformed.) However the z_j corresponding to a particular s_j might have to be calculated by the use of the second branch of $\ln z(s)$. We therefore obtain

$$2\pi i \sum_j \ln z(s_j) = \int_{\mathcal{L}_0} f(s)\big|_{1.\text{branch}} ds + \int_{\mathcal{L}_0} f(s)\big|_{2.\text{branch}} ds, \tag{78}$$

where the first and second term on the right hand side will be abbreviated by Σ_1 and Σ_2, respectively. We next manipulate Σ_1

$$\begin{aligned} \Sigma_1 &= \int_{\mathcal{L}_0 \equiv -(\mathcal{L}_1+\mathcal{L}_2+\mathcal{L}_3)} \ln z(s) \left[\ln\left(1 + \frac{l_4}{l_3}(s)\right)\right]' ds, \\ &= -\int_{\mathcal{L}_1+\mathcal{L}_3} \ln z(s) \left[\ln\left(1 + \frac{l_4}{l_3}(s)\right)\right]' ds + \int_{\mathcal{L}_2} \ln z(s) \left[\ln \overline{T}(s)\right]' ds, \end{aligned} \tag{79}$$

where in the first line the integration contour $\mathcal{L}_0$ can be replaced due to Cauchy's theorem by three contours (taken in anticlockwise manner): $\mathcal{L}_1$ from $i\infty$ to -1, surrounding $[-1, 1]$, from -1 back to $i\infty$; $\mathcal{L}_2$ surrounding the axis $\mathrm{Im}(s) = -\gamma$ (where the simple poles of $[1 + l_4/l_3(s)]$ are located, which are identical to the simple zeros of $\overline{T}(s)$); $\mathcal{L}_3$ around s_0 (which is a pole of order $N/2$ of $[1 + l_4/l_3(s)]$), see (31). Next we replace $\mathcal{L}_2$ by contours $\mathcal{L}_1$, $\mathcal{L}-2i\gamma$ (where $\mathcal{L}$ surrounds the real axis), and $\mathcal{L}_3-2i\gamma$

$$\begin{aligned} \int_{\mathcal{L}_2} \ln z(s) \left[\ln \overline{T}(s)\right]' ds = &- \int_{\mathcal{L}_1} \ln z(s) \left[\ln \overline{T}(s)\right]' ds \\ &- \int_{\mathcal{L}_3+\mathcal{L}} \ln z(s-2i\gamma) \left[\ln \overline{T}(s-2i\gamma)\right]' ds. \end{aligned} \tag{80}$$

In the last term of (80) the function $\ln \overline{T}(s - 2i\gamma)$ can be replaced by $-\ln \mathfrak{B}(s)$ as the difference of these functions amounts to an analytic contribution vanishing in the contour integration. Of course, the $\mathcal{L}_3$ integration in (79) and (80) can be done explicitly yielding

$$\begin{aligned} \Sigma_1 = &\pi i N \ln[z(s_0) z(s_0 - 2i\gamma)] \\ &- \int_{\mathcal{L}_1} \ln z(s) \left[\ln\left(\overline{T}(s)\left(1 + \frac{l_4}{l_3}(s)\right)\right)\right]' ds + \int_{\mathcal{L}} \ln z(s-2i\gamma) \left[\ln \mathfrak{B}(s)\right]' ds. \end{aligned} \tag{81}$$

Next we perform integration by parts on the right hand side where the first integral also contributes a "surface term"

$$\begin{aligned}\Sigma_1 = &-2\pi i \ln\left[\left(1+\mathrm{e}^{-\beta(\mu+H/2)}\right)\left(1+\mathrm{e}^{\beta(\mu-H/2)}\right)\right] + \pi i N \ln[z(s_0)z(s_0-2i\gamma)] \\ &+ \int_{\mathcal{L}_1} [\ln z(s)]' \ln\left[\overline{T}(s)\left(1+\frac{l_4}{l_3}(s)\right)\right] ds - \int_{\mathcal{L}} [\ln z(s-2i\gamma)]' \ln \mathfrak{B}(s) ds,\end{aligned} \tag{82}$$

where now the integration along $\mathcal{L}_1$ can be restricted to a loop $\mathcal{L}_4$ along the cut from -1 to 1. In the limit $N \to \infty$ we can replace $\pi i N \ln[z(s_0)z(s_0-2i\gamma)]$ by $2\pi i N \ln z_-(w) + 4\pi i\beta\gamma$ such that in combination with (24)

$$\begin{aligned}2\pi i \ln\Lambda = 2\pi i\beta(\mu+H/2+U/4) + \Sigma_2 &+ \int_{\mathcal{L}_4} [\ln z(s)]' \ln\left[\overline{T}(s)\left(1+\frac{l_4}{l_3}(s)\right)\right] ds \\ &- \int_{\mathcal{L}} [\ln z(s-2i\gamma)]' \ln \mathfrak{B}(s) ds.\end{aligned} \tag{83}$$

A very similar line of reasoning yields

$$\begin{aligned}2\pi i \ln\Lambda = 2\pi i\beta(\mu-H/2+U/4) + \Sigma_2' &+ \int_{\mathcal{L}_4} [\ln z(s)]' \ln\left[T(s)\left(1+\frac{l_3}{l_4}(s)\right)\right] ds \\ &- \int_{\mathcal{L}} [\ln z(s+2i\gamma)]' \ln \overline{\mathfrak{B}}(s) ds,\end{aligned} \tag{84}$$

where Σ_2' is defined similarly to Σ_2 after interchanging l_3 and l_4. Combining (83,84) we find the symmetrised version

$$\begin{aligned}4\pi i \ln\Lambda =& 4\pi i\beta(\mu+U/4) + \Sigma_2 + \Sigma_2' \\ &+ \int_{\mathcal{L}_4} [\ln z(s)]' \ln\left[T(s)\overline{T}(s)\left(1+\frac{l_4}{l_3}(s)\right)\left(1+\frac{l_3}{l_4}(s)\right)\right] ds \\ &- \int_{\mathcal{L}} [\ln z(s-2i\gamma)]' \ln \mathfrak{B}(s) ds - \int_{\mathcal{L}} [\ln z(s+2i\gamma)]' \ln \overline{\mathfrak{B}}(s) ds.\end{aligned} \tag{85}$$

The present formula is still inconvenient as the first terms on the right hand side contain "non-standard" functions. However, we can substitute the terms

$$\left[\left(1+\frac{l_4}{l_3}(s)\right)\left(1+\frac{l_3}{l_4}(s)\right)\right]\Big|_{\text{1.branch}} \longrightarrow \left[\left(1+\frac{l_4}{l_3}(s)\right)\left(1+\frac{l_3}{l_4}(s)\right)\right]\Big|_{\text{2.branch}} \tag{86}$$

without change of the integral as $[\ln z(s)]'|_{\text{1.branch}} = -[\ln z(s)]'|_{\text{2.branch}}$. For the same reason we find

$$\begin{aligned}\Sigma_2 + \Sigma_2' &= -\int_{\mathcal{L}_0} \left([\ln z(s)]' \ln\left[\left(1+\frac{l_4}{l_3}(s)\right)\left(1+\frac{l_3}{l_4}(s)\right)\right]\right)\Big|_{\text{2.branch}} ds \\ &= \int_{\mathcal{L}_0} [\ln z(s)]' \ln\left[\left(1+\frac{l_4}{l_3}(s)\right)\left(1+\frac{l_3}{l_4}(s)\right)\right]\Big|_{\text{2.branch}} ds,\end{aligned} \tag{87}$$

where functions have to be evaluated on the 1. branch unless indicated differently. Inserting (86,87) into (85), combining the contours $\mathcal{L}_0$ and $\mathcal{L}_4$ into $\mathcal{L}$, and simply extending $\mathcal{L}_4$ to $\mathcal{L}$ for the integrals involving T and $\overline{T}$ (due to analyticity) we arrive at

$$\begin{aligned} 4\pi i \ln\Lambda =& 4\pi i\beta(\mu+U/4) \\ &+ \int_{\mathcal{L}} [\ln z(s)]' \ln\left[T(s)\overline{T}(s) \left(\left(1+\frac{l_4}{l_3}(s)\right)\left(1+\frac{l_3}{l_4}(s)\right)\right)\Big|_{\text{2.branch}}\right] ds \\ &- \int_{\mathcal{L}} [\ln z(s-2i\gamma)]' \ln \mathfrak{B}(s) ds - \int_{\mathcal{L}} [\ln z(s+2i\gamma)]' \ln \overline{\mathfrak{B}}(s) ds. \end{aligned} \tag{88}$$

Next we find the identity

$$(l_4/l_3)\,\big|_{\text{2.branch}} = \left(\mathfrak{b}T/\overline{T}\right)\big|_{\text{1.branch}} \tag{89}$$

Hence the integrand of the first integral in (88) is

$$T\overline{T}\left[\left(1+\frac{\mathfrak{b}T}{\overline{T}}\right)\left(1+\frac{\overline{T}}{\mathfrak{b}T}\right)\right] = \frac{(\overline{T}+\mathfrak{b}T)^2}{b} = (1+\mathfrak{c}+\overline{\mathfrak{c}})^2\mathfrak{B}\overline{\mathfrak{B}}, \tag{90}$$

with all functions on the first branch. We are now in the position to formulate the first main expression for the eigenvalue

$$\begin{aligned} 4\pi i\ln\Lambda =& 4\pi i\beta(\mu+U/4) + 2\int_{\mathcal{L}} [\ln z(s)]' \ln\left(1+\mathfrak{c}+\overline{\mathfrak{c}}\right) ds \\ &- \int_{\mathcal{L}} \left[\ln\frac{z(s-2i\gamma)}{z(s)}\right]' \ln\mathfrak{B}(s) ds - \int_{\mathcal{L}} \left[\ln\frac{z(s+2i\gamma)}{z(s)}\right]' \ln\overline{\mathfrak{B}}(s) ds. \end{aligned} \tag{91}$$

The last equation can be reduced further by substituting the $\overline{\mathfrak{B}}$ integral by a $\mathfrak{B}$ integral. For this purpose we employ (29)

$$\begin{aligned} &\int_{\mathcal{L}} \left[\ln\frac{z(s+2i\gamma)}{z(s)}\right]' \ln\overline{\mathfrak{B}}(s) ds \\ &\quad= \int_{\mathcal{L}} \left[\ln\frac{z(s+2i\gamma)}{z(s)}\right]' \ln(l_1+l_2+l_3+l_4+\overline{l_1}+\overline{l_2}+\overline{l_3}+\overline{l_4}) ds \\ &\quad- \int_{\mathcal{L}} \left[\ln\frac{z(s+2i\gamma)}{z(s)}\right]' \ln(\overline{l_1}+\overline{l_2}+\overline{l_3}+\overline{l_4}) ds. \end{aligned} \tag{92}$$

In the first term on the right hand side the contribution due to $z(s+2i\gamma)$ vanishes upon taking the contour integral and can be replaced by (the equally vanishing) $z(s-2i\gamma)$. In the second term the contour is replaced by $-(\mathcal{L}-2i\gamma)$. Using $(\overline{l_1}+\overline{l_2}+\overline{l_3}+\overline{l_4})(s-2i\gamma) = \exp(-\beta H)(l_1+l_2+l_3+l_4)(s)/[\phi^+(s)\phi^-(s)]$ we find

$$\begin{aligned} &\int_{\mathcal{L}\equiv-(\mathcal{L}-2i\gamma)} \left[\ln\frac{z(s+2i\gamma)}{z(s)}\right]' \ln(\overline{l_1}+\overline{l_2}+\overline{l_3}+\overline{l_4}) ds \\ &\qquad= 2\pi i\beta H + \int_{\mathcal{L}} \left[\ln\frac{z(s-2i\gamma)}{z(s)}\right]' \ln(l_1+l_2+l_3+l_4) ds, \end{aligned} \tag{93}$$

where terms involving $\phi^+\phi^-$ have been dropped as they vanish in the limit $N \to \infty$. Inserting this into (92) we obtain

$$\int_{\mathcal{L}} \left[\ln \frac{z(s+2i\gamma)}{z(s)}\right]' \ln \overline{\mathfrak{B}}(s) ds = -2\pi i\beta H + \int_{\mathcal{L}} \left[\ln \frac{z(s-2i\gamma)}{z(s)}\right]' \ln \mathfrak{B}(s) ds, \tag{94}$$

and with (91) we find

$$\begin{aligned} 2\pi i \ln \Lambda = 2\pi i\beta(\mu + H/2 + U/4) + \int_{\mathcal{L}} [\ln z(s)]' \ln\left(1 + \mathfrak{c} + \overline{\mathfrak{c}}\right) ds \\ - \int_{\mathcal{L}} \left[\ln \frac{z(s-2i\gamma)}{z(s)}\right]' \ln \mathfrak{B}(s) ds. \end{aligned} \tag{95}$$

Finally, we want to show how to express the eigenvalue entirely in terms of $\mathfrak{c}$ functions, i.e. without contributions by $\mathfrak{b}$. To this end we note the identity

$$\begin{aligned} \int_{\mathcal{L}\equiv -(\mathcal{L}-2i\gamma)} [\ln z(s)]' \ln \overline{\tau}(s) ds = -2\pi i\beta(\mu + H/2 + U/2) \\ - \int_{\mathcal{L}} [\ln z(s-2i\gamma)]' \ln \overline{\tau}(s-2i\gamma) ds, \end{aligned} \tag{96}$$

where we have dropped terms that do not contribute in the limit $N \to \infty$. Next we replace the $\overline{\tau}(s)$ and $\overline{\tau}(s-2i\gamma)$ functions by

$$\overline{\tau} = \overline{\mathfrak{c}}\mathfrak{B}, \qquad [\overline{\tau}(s-2i\gamma)]^{-1} = \tau(s) = \frac{l_1 + l_2}{l_3 + l_4 + \overline{l_1} + \overline{l_2} + \overline{l_3} + \overline{l_4}} \mathfrak{B}\mathfrak{C}. \tag{97}$$

Since the function $(l_1 + l_2)/(l_3 + l_4 + \overline{l_1} + \overline{l_2} + \overline{l_3} + \overline{l_4})$ is analytic in the neighborhood of the real axis its contribution to (96) vanishes. Therefore (96) results into

$$\begin{aligned} \int_{\mathcal{L}} [\ln z(s)]' (\ln \overline{\mathfrak{c}}(s) + \ln \mathfrak{B}(s)) ds = -2\pi i\beta(\mu + H/2 + U/2) \\ + \int_{\mathcal{L}} [\ln z(s-2i\gamma)]' (\ln \mathfrak{B}(s) + \ln \mathfrak{C}(s)) ds. \end{aligned} \tag{98}$$

Inserting this into (95) we are left with

$$2\pi i \ln \Lambda = -2\pi i\beta \frac{U}{4} + \int_{\mathcal{L}} [\ln z(s)]' \ln \frac{1 + \mathfrak{c} + \overline{\mathfrak{c}}}{\overline{\mathfrak{c}}} ds + \int_{\mathcal{L}} [\ln z(s-2i\gamma)]' \ln \mathfrak{C}(s) ds. \tag{99}$$

References

[1] E.H. Lieb and F.Y. Wu, Phys. Rev. Lett. 20 (1968) 1445.

[2] A. Ovchinnikov, Soviet Phys. JETP 30 (1970) 1160.

[3] C. Coll, Phys. Rev. B 9 (1974) 2150.

[4] F. Woynarovich, J. Phys. A 15 (1982) 2985.

[5] A. Klümper, A. Schadschneider and J. Zittartz, Z. Physik B 78 (1990) 99.

[6] H. Shiba, Phys. Rev. B 6 (1972) 930.

[7] M.Ogata and H.Shiba, Phys. Rev. B 41 (1990) 2326.

[8] F. Essler, V. Korepin and K. Schoutens, Phys. Rev. Lett. 67 (1991) 3848.

[9] D. Uglov and V. Korepin, Phys. Lett. A 190 (1994) 238.

[10] S. Murakami and F. Göhmann, Phys. Lett. A 227 (1997) 216.

[11] C. Yang, Phys. Rev. Lett. 63 (1989) 2144.

[12] H. Frahm and V.E. Korepin, Phys. Rev. B 42 (1990) 10553.

[13] H. Frahm and V.E. Korepin, Phys. Rev. B 43 (1991) 5653.

[14] F. Woynarovich, J. Phys. A 22 (1989) 4243.

[15] H. Schultz, Int. J. Mod. Phys. B 5 (1991) 57.

[16] M. Takahashi, Prog. Theor. Phys. 47 (1972) 69.

[17] N. Kawakami, T. Usuki and A. Okiji, Phys. Lett. A 37 (1989) 287.

[18] T. Usuki, N. Kawakami and A. Okiji, J. Phys. Soc. Japan 59 (1990) 1357.

[19] M. Suzuki, Phys. Rev. B 31 (1985) 2957.

[20] M. Suzuki and M. Inoue, Prog. Theor. Phys. 78 (1987) 787.

[21] T. Koma, Prog. Theor. Phys. 78 (1987) 1213.

[22] J. Suzuki, Y. Akutsu and M. Wadati, J. Phys. Soc. Japan 59 (1990) 2667.

[23] K. Tsunetsugu, J. Phys. Soc. Japan 60 (1991) 1460.

[24] M. Takahashi, Phys. Rev. B 43 (1991) 5788, see also vol. 44 p. 12382.

[25] A. Klümper, Ann. Physik 1 (1992) 540.

[26] A. Klümper, Z. Physik B 91 (1993) 507.

[27] C. Destri and H.J. de Vega, Phys. Rev. Lett. 69 (1992) 2313.

[28] J. Suzuki, T. Nagao and M. Wadati, Int. J. Mod. Phys. B 6 (1992) 1119.

[29] G. Jüttner and A. Klümper, Euro. Phys. Letts. 37 (1997) 335.

[30] G. Jüttner, A. Klümper and J. Suzuki, Nucl. Phys. B 486 (1997) 650.

[31] G. Jüttner, A. Klümper and J. Suzuki, J. Phys. A 30 (1997) 1181.

[32] R.Z. Bariev, Theor. and Math. Phys. 49 (1981) 1021.

[33] A. Klümper and R.Z. Bariev, Nucl. Phys. B 458 (1996) 623.

[34] B.S. Shastry, J. Stat. Phys. 50 (1988) 57.

[35] E. Olmedilla, M. Wadati and Y. Akutsu, J. Phys. Soc. Japan 56 (1987) 2298.

[36] M. Wadati, E. Olmedilla and Y. Akutsu, J. Phys. Soc. Japan 56 (1987) 1340.

[37] B. Sutherland, Phys. Rev. B 12 (1975) 3795.

[38] P. Schlottmann, Phys. Rev. B 36 (1987) 5177.

[39] P.A. Bares, G. Blatter and M. Ogata, Phys. Rev. B 44 (1991) 130.

[40] B.S. Shastry, Phys. Rev. Lett. 56 (1986) 1529.

[41] M. Shiroishi and M. Wadati, J. Phys. Soc. Japan 64 (1995) 57.

[42] P. Ramos and M. Martins, J. Phys. A 30 (1997) L195.

[43] R.H. Yue and T. Deguchi, J. Phys. A 30 (1997) 849.

[44] A. Klümper and M.T. Batchelor, J. Phys. A 23 (1990) L189.

[45] A. Klümper, M.T. Batchelor and P.A. Pearce, J. Phys. A 24 (1991) 3111.

[46] Y. Kato and Y. Kuramoto, J. Phys. Soc. Japan 65 (1996) 1622.

[47] F. Gebhard, A. Girndt and A.E. Ruckenstein, Phys. Rev. B 49 (1994) 10926.

[48] H.Shiba, Prog. Theor. Phys. 48 (1972) 2171.

[49] J. des Cloizeaux and J.J. Pearson, Phys. Rev. 128 (1962) 2131.

[50] J. Johnson, S. Krinsky and B. McCoy, Phys. Rev. A 8 (1973) 2526.

[51] L. Faddeev and L. Takhtajan, Phys. Lett. A 85 (1981) 375.

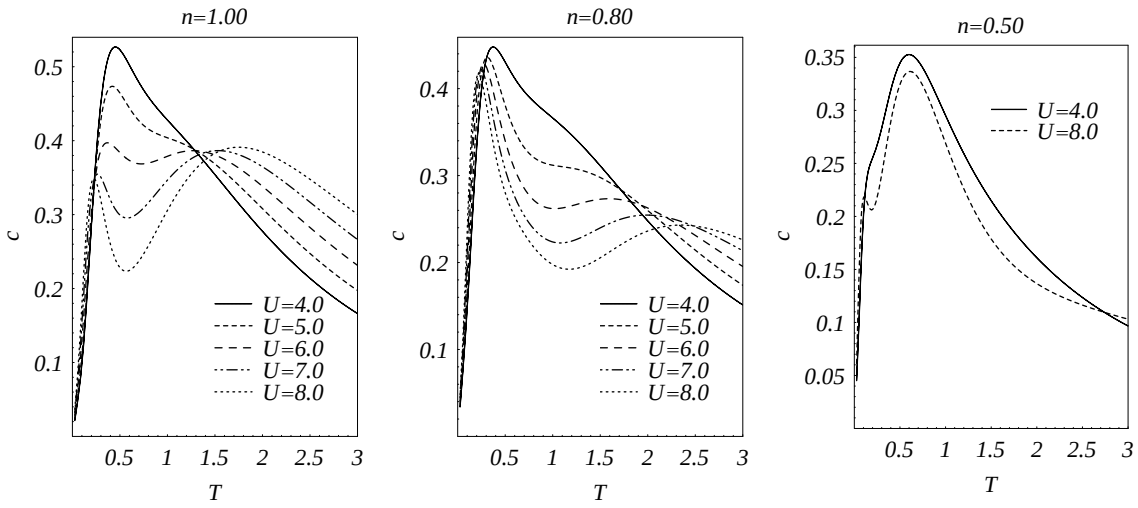

Figure 3: Specific heat versus T for particle densities $n = 1$, $n = 0.8$ and $n = 0.5$.

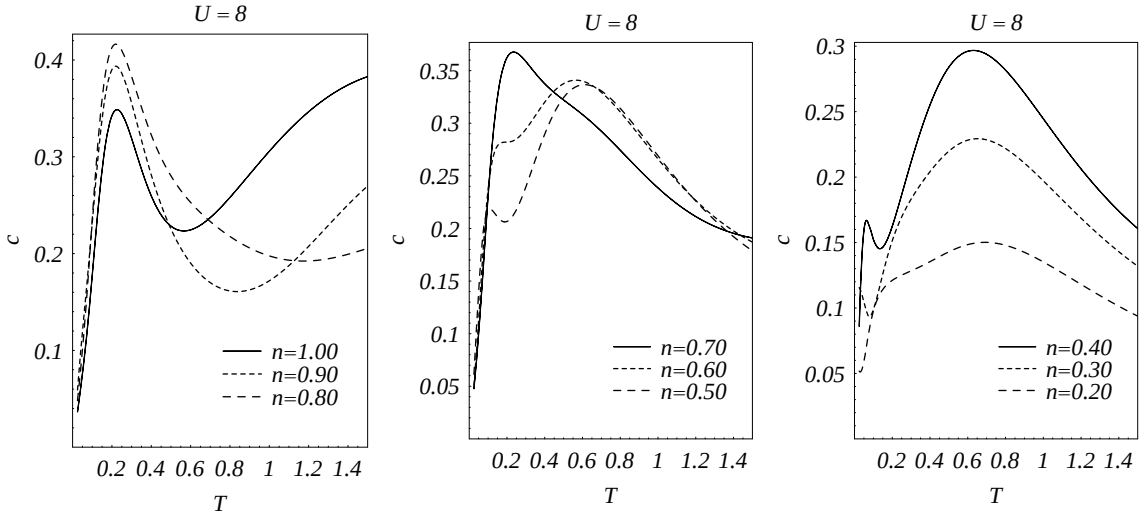

Figure 4: Specific heat versus T for fixed $U = 8$.

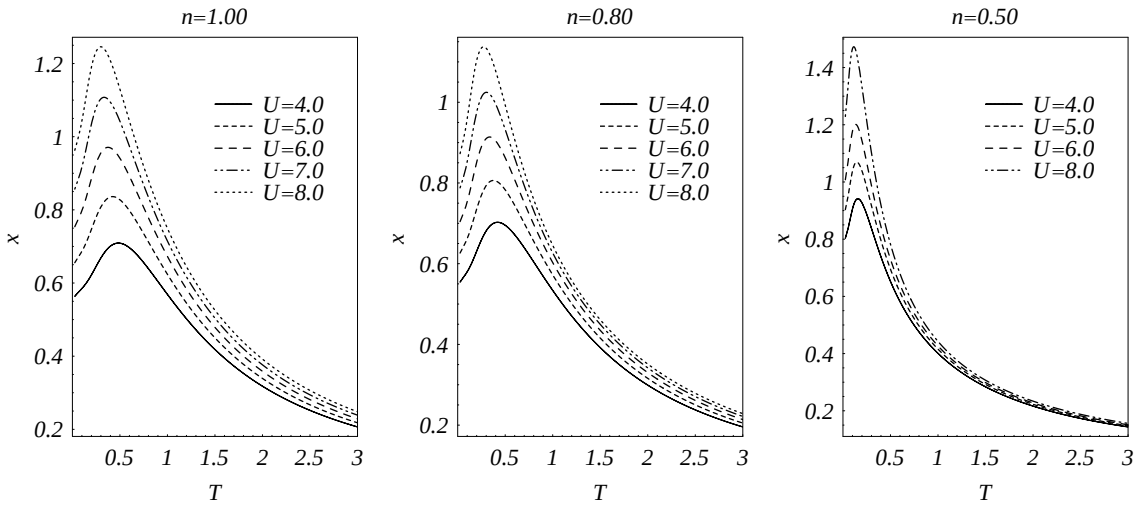

Figure 5: Magnetic susceptibility versus T for $n = 1$, $n = 0.8$ and $n = 0.5$.

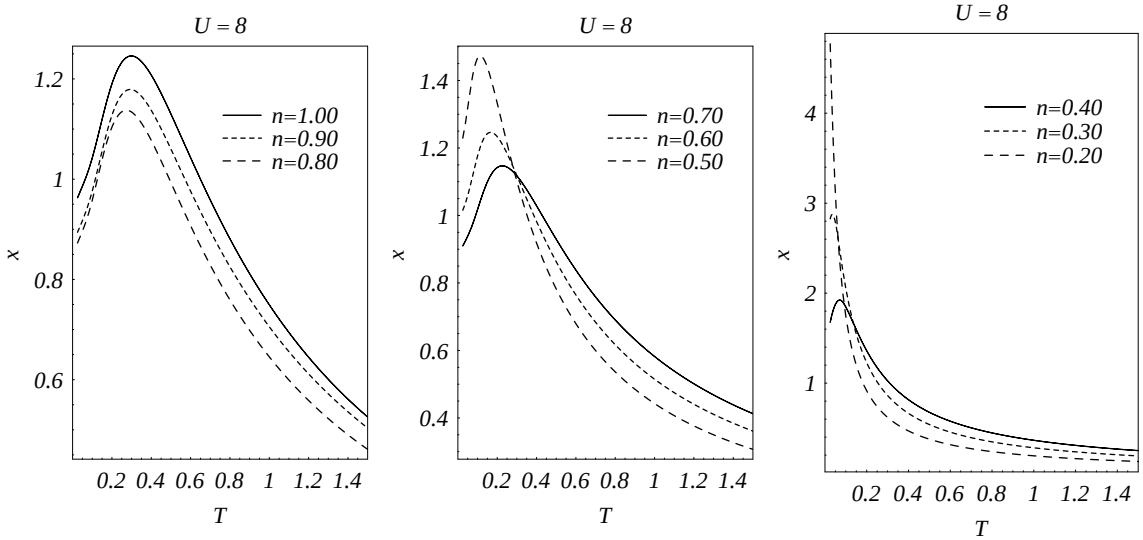

Figure 6: Magnetic susceptibility versus T for fixed $U = 8$.

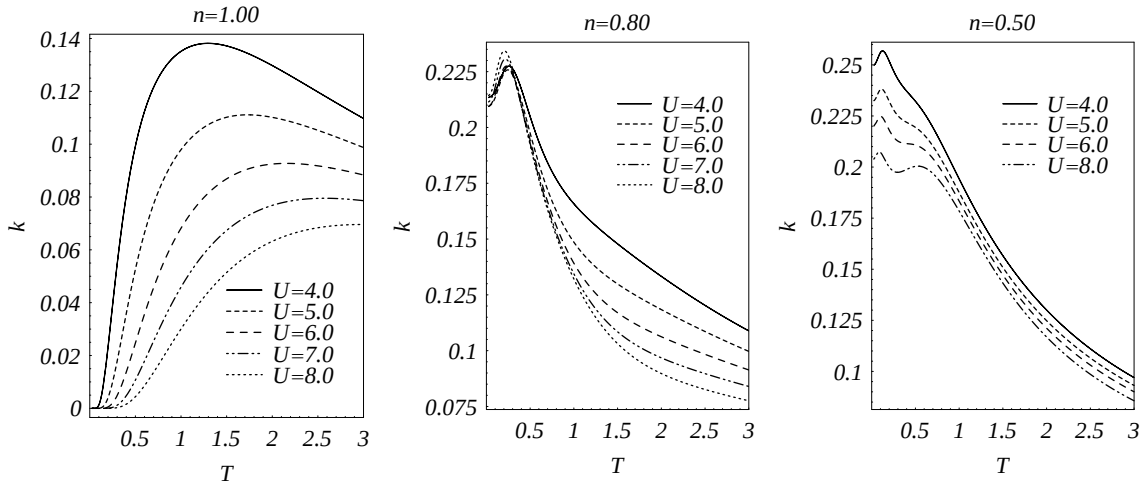

Figure 7: Compressibility versus T for particle densities $n = 1$, $n = 0.8$ and $n = 0.5$.

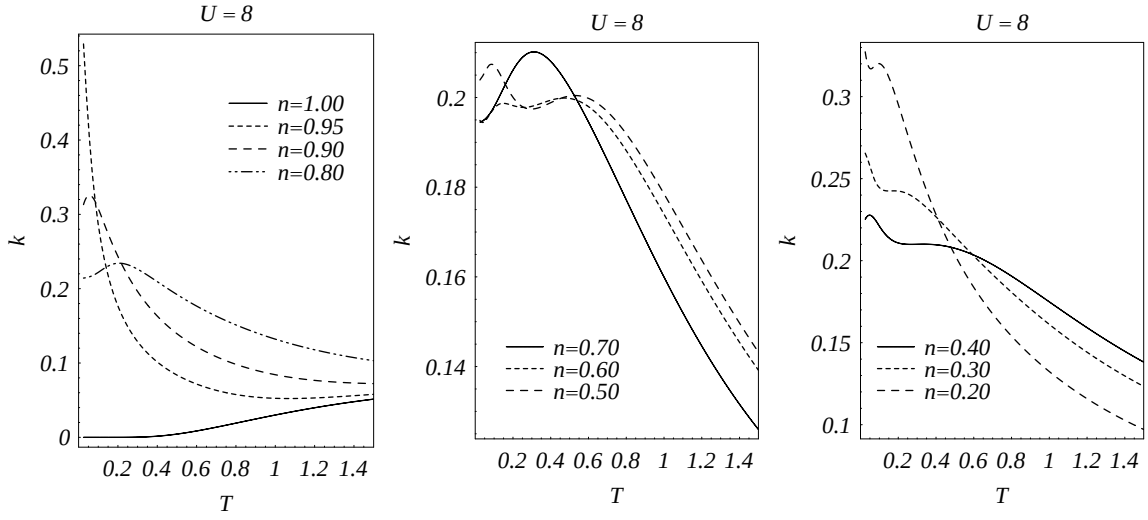

Figure 8: Compressibility versus T for fixed $U = 8$.

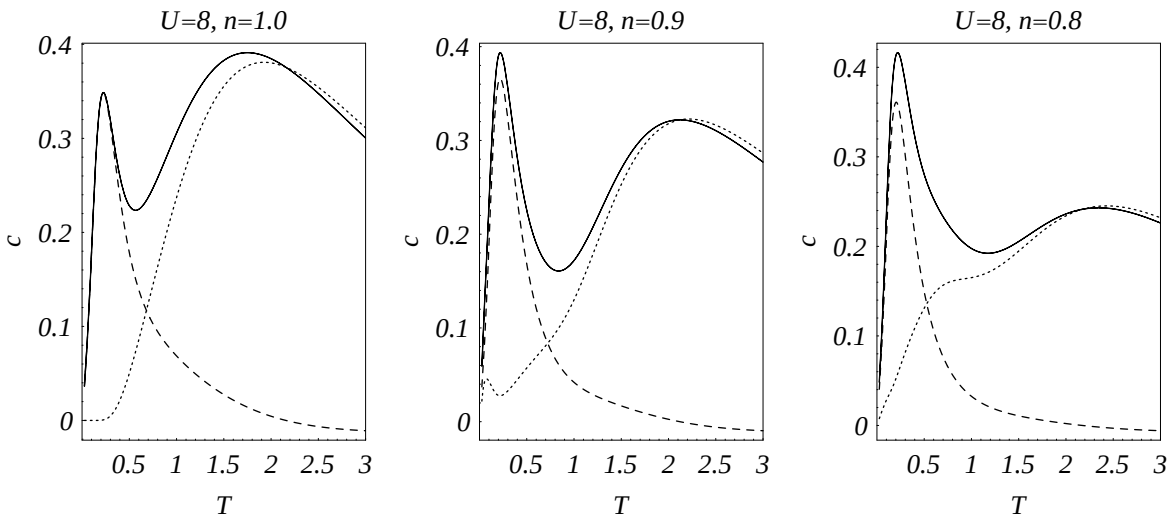

Figure 9: Separation of specific heat (solid) in spin (dashed) and charge components (dotted).